Cerebral Cortex March 2015;25:680–702
doi:10.1093/cercor/bht260
Advance Access publication September 24, 2013

Large-Scale Brain Networks of the Human Left Temporal Pole: A Functional Connectivity MRI Study

Belen Pascual[1], Joseph C. Masdeu[2], Mark Hollenbeck[1], Nikos Makris[3,4], Ricardo Insausti[5], Song-Lin Ding[6] and Bradford C. Dickerson[1,4]

[1]MGH Frontotemporal Dementia Unit, Alzheimer's Disease Research Center, Department of Neurology, Martinos Center for Biomedical Imaging, Massachusetts General Hospital and Harvard Medical School, Charlestown, MA 02129, USA, [2]Section on Integrative Neuroimaging, National Institutes of Health, Bethesda, MD 20892, USA, [3]Center for Morphometric Analysis, Departments of Psychiatry, Neurology, and Radiology Services, [4]Center for Neural Systems Investigation, Departments of Neurology and Psychiatry, Massachusetts General Hospital and Harvard Medical School, Charlestown, MA 02129, USA, [5]Center for Human Neuroanatomy Laboratory, Department of Health Sciences, School of Medicine, University of Castilla-La Mancha, Albacete 02071, Spain and [6]Allen Institute for Brain Science, Seattle, WA 98103, USA

Address correspondence to Dr Bradford C. Dickerson, MGH Frontotemporal Dementia Unit, 149 13th St., Suite 2691, Charlestown, MA 02129, USA. Email: bradd@nmr.mgh.harvard.edu

The most rostral portion of the human temporal cortex, the temporal pole (TP), has been described as "enigmatic" because its functional neuroanatomy remains unclear. Comparative anatomy studies are only partially helpful, because the human TP is larger and cytoarchitectonically more complex than in nonhuman primates. Considered by Brodmann as a single area (BA 38), the human TP has been recently parceled into an array of cytoarchitectonic subfields. In order to clarify the functional connectivity of subregions of the TP, we undertook a study of 172 healthy adults using resting-state functional connectivity MRI. Remarkably, a hierarchical cluster analysis performed to group the seeds into distinct subsystems according to their large-scale functional connectivity grouped 87.5% of the seeds according to the recently described cytoarchitectonic subregions of the TP. Based on large-scale functional connectivity, there appear to be 4 major subregions of the TP: 1) dorsal, with predominant connectivity to auditory/somatosensory and language networks; 2) ventromedial, predominantly connected to visual networks; 3) medial, connected to paralimbic structures; and 4) anterolateral, connected to the default-semantic network. The functional connectivity of the human TP, far more complex than its known anatomic connectivity in monkey, is concordant with its hypothesized role as a cortical convergence zone.

Keywords: anterior temporal lobe, brain anatomy, cytoarchitecture, language, resting-state fMRI

Introduction

Since Arnold Pick's pioneering clinicopathologic studies of patients with progressive aphasia and behavioral symptoms (Pick 1905) and Klüver and Bucy's ablation experiments in monkeys (Klüver and Bucy 1939), the temporal pole (TP) has been known to play an important role in language, visual cognition, and socioaffective behavior. In addition to frontotemporal dementia, as Pick's disease is now called, the TP is affected in Alzheimer's disease (AD), traumatic brain injury, herpes encephalitis, and temporal lobe epilepsy (Kapur et al. 1994; Thompson et al. 2003; Chabardes et al. 2005; Bigler 2007; Dickerson et al. 2009, 2011). The TP is not commonly lesioned in patients with strokes, and when it is, a large portion of the left hemisphere is usually involved as well, thus confounding the correlation of the anatomy with behavior (Phan et al. 2009). Contemporary investigations of patients with TP lesions as a result of one of these disorders have highlighted its importance in semantic and lexical skills (Damasio et al. 1996; Mummery et al. 2000; Patterson 2007; Wilson et al. 2010), face recognition (Damasio et al. 1990; Evans et al. 1995), other high-level visual and auditory processing as well as semantic memory (Horel et al. 1975; Fukatsu et al. 1999; Glosser et al. 2003; Lambon Ralph et al. 2011), socioaffective behavior including empathy (Damasio et al. 2000; Gorno-Tempini et al. 2004), and the regulation of eating and sexual behavior (Marlowe et al. 1975; Lilly et al. 1983; Anson and Kuhlman 1993). Despite these compelling clinical observations, the functional–anatomic organization of the human TP is so poorly understood that it has been dubbed "the enigmatic TP" (Olson et al. 2007).

The human TP has recently attracted renewed interest because functional neuroimaging studies have provided a more refined understanding of its role in many complex behaviors. The TP is involved in semantic (Binder et al. 1999; Sharp et al. 2004; Visser and Lambon Ralph 2011) and conceptual processing (Baron and Osherson 2011), the analysis of musical melody (Griffiths et al. 1998), the identification of speakers by listening to their voice (Imaizumi et al. 1997), face, and name association skills (Gorno-Tempini et al. 1998; Tsukiura et al. 2006), and social or theory of mind tasks (Fletcher et al. 1995; Zahn et al. 2007). Careful examination of these experiments reveals that these abilities map mainly onto the dorsal aspect of the TP. In contrast, the ventral aspect of TP seems to play a role in higher order visual processing (Allison et al. 1999), such as face familiarity judgments (Nakamura et al. 2000), and identifying the emotional valence of faces (Blair et al. 1999; Royet et al. 2000); as well as in integrating visual and auditory information in semantic tasks (Visser et al. 2012). In addition, this region is involved in numerous aspects of emotional processing, including the subjective perception of affect (Shin et al. 2000; Mathiak et al. 2011) as well as anxiety and stress (Kimbrell et al. 1999; Tillfors et al. 2001). In summary, the ventral TP seems to play a role in integrating visual information and viscero-autonomic responses, as suggested by its description as a key region of the paralimbic cortex (Mesulam 2000). The different functions of the dorsal and ventral portions of the TP indicate that this brain region is likely to contain functional subunits (Skipper et al. 2011).

With respect to its structural anatomy, for many decades, the TP had been described as a single cortical area, based mostly

on cyto- and myeloarchitectonic studies. It was initially called planum polare by Smith (1907), area 38 by Brodmann (1909), or area TG by von Economo and Koskinas (1925) and von Economo (1929). Using more sophisticated techniques, including immunochemical detection of neurochemical markers, morphologists have begun to dissect the TP into multiple subregions (Insausti et al. 1998; Blaizot et al. 2010). Ding et al. (2009) have provided strong cytoarchitectonic evidence that the human TP contains at least 7 different areas: 1) a dysgranular area capping the rostral tip of the TP which they name TG) dorsocaudal to it, on the anterior extent of the superior temporal gyrus, there are areas 2) TAr and 3) TAp; 4) caudolateral to TG is area TE; on the medial surface are areas 5) anterior area 36 and 6) anterior area 35, dorsal to which is 7) area TI. As with all other paralimbic–isocortical zones, the transition between these areas is gradual. Besides capturing many distinct cellular and molecular structural features within the TP, Ding et al. postulate that this more nuanced anatomical description may better explain the diverse functions of the human TP.

To clarify these functions, an understanding of the connectivity of the TP is essential. In this regard, tract-tracing studies of TP connectivity in the macaque have contributed substantially, but this species has a comparatively smaller and simpler TP than that found in humans;, for example, the macaque lacks a middle temporal gyrus (Nakamura and Kubota 1996; Blaizot et al. 2010). As in humans, 3 general types of cortex are recognized in the TP of the macaque (Moran et al. 1987; Nakamura and Kubota 1996; Kondo et al. 2003): agranular, dysgranular, and granular cortices. Macaque TP subregions have distinct anatomical connections with prefrontal cortex, temporal cortex, amygdala, and insula (Mesulam and Mufson 1982; Mufson and Mesulam 1982; Markowitsch et al. 1985; Moran et al. 1987; Kondo et al. 2003, 2005; Hoistad and Barbas 2008). Recently, diffusion-weighted imaging tractography has shown a connectivity pattern of the human TP that suggests its role as a convergence hub, with important implications in language and multimodal semantic processing (Binney et al. 2012).

In the present study, we used functional MRI (fMRI) resting-state functional connectivity (RSFC) analysis to map the topography of in vivo large-scale functional–anatomic networks anchored in the human TP. The goal of the present study was to use a systems neuroanatomic approach to refine our understanding of the organization and likely functions of specific regions within the human TP. We approached this question by performing a comprehensive mapping of the functional connectivity of the human TP and identifying clusters of TP regions with similar or distinct large-scale cortical and subcortical connectivity patterns. We sought to compare the connectional topography of human TP subregions with the anatomical connectivity demonstrated by tract-tracing studies in the macaque monkey (Moran et al. 1987; Nakamura and Kubota 1996; Kondo et al. 2003). Furthermore, we hypothesized that the clustering of the large-scale connectivity patterns of seed points within the TP would reflect the recently described cytoarchitectonic subdivisions of the human TP (Ding et al. 2009).

Materials and Methods

The present study has 3 components. First, in human healthy volunteers, we used resting fMRI to analyze the functional connectivity of seed regions in the left TP to the entire brain. The seeds were arranged in a regular geometrical array, without consideration of cytoarchitectonics. Then, we grouped the connectivity patterns obtained from the different seeds using an unbiased hierarchical cluster analysis; the location of the groups of seeds with similar connectivity was then compared with the recent cytoarchitectonic parcellation of the TP by Ding et al. (2009). Finally, we performed a comprehensive review of the tract-tracing literature describing anatomical connectivity of the TP in the rhesus macaque.

Participants

Data from 172 healthy adults (98 females; ages 18–35 years, mean age: 22.9 ± 3.4 years) from 3 different samples was first grouped into 2 independent datasets, of 89 (Dataset 1) and 83 (Dataset 2) subjects. Once the reliability analysis was performed, the 2 datasets were pooled into a single large sample. Demographic data for each sample are listed in Table 1. All participants had normal or corrected-to-normal vision and were right-handed, native English speakers. No participant reported a history of a neurological or psychiatric disorder. Informed consent was obtained in accordance with guidelines set forth by the institutional review board of the Massachusetts General Hospital and Partners Healthcare System Human Research Committee.

fMRI Data Acquisition and Preprocessing Procedures

All participants were scanned at the Athinoula A. Martinos Center for Biomedical Imaging, Massachusetts General Hospital (Charlestown, MA), using a 3 Tesla Tim Trio scanner (Siemens Medical Systems, Erlangen, Germany), equipped with a 32-channel phased-array head coil. Whole brain resting-state fMRI (rs-fMRI) data were acquired using a T_2*-weighted gradient-echo echo-planar sequence. Structural images were acquired for registration purposes using a high-resolution T_1-weighted magnetization-prepared gradient-echo sequence. Parameters for the rs-fMRI and structural sequences for the 3 samples are listed in Supplementary Table 1. During the rs-fMRI runs, acquired for 6 min before task runs, in a standard fashion, participants were instructed to keep their eyes open. Cushions and clamps were used to minimize head movement during scanning, and scanner noise was attenuated with earplugs.

A series of preprocessing steps were used to remove spurious variance and prepare the rs-fMRI data for statistical analysis (Biswal et al. 1995; Vincent et al. 2006; Van Dijk et al. 2010). The first 4 volumes were removed to allow for T_1-equilibration effects. Using SPM2 software (Welcome Department of Cognitive Neurology, London, United Kingdom), data were corrected for differences in acquisition time between interleaved slices for each whole-brain volume. Head motion correction was obtained with rigid-body transformation using 3 translations and 3 rotations within and across runs (FMRIB, Oxford, UK). Next, affine transforms were generated, which connected the first volume of the first functional run to the T_1-weighted structural images (FMRIB). Using SPM2, data were then transformed to align with the Montreal Neurological Institute (MNI) atlas space. Motion correction and atlas transformations were applied to produce motion-corrected functional time series volumes with 2 mm cubic voxels. A low-pass temporal filter was used to remove frequencies above 0.08 Hz. Spatial

Table 1
Demographics of the participants

	N	Gender (male/female)	Age (mean ± SD)	Age range (years)
Dataset 1				
Sample 1	89	44/45	22.2 ± *3.3*	18–33
Total	**89**	**44/45**	**22.2 ± 3.3**	**18–33**
Dataset 2				
Sample 2	65	24/41	23.7 ± 3.4	18–35
Sample 3	18	6/12	23.7 ± *2.7*	19–31
Total	**83**	**30/53**	**23.7 ± 3.1**	**18–35**

Dataset 1 includes only sample 1. Dataset 2 includes samples 2 and 3. Bolded are each dataset characteristics.

filtering was obtained with a 6 mm full-width half-maximum Gaussian filter. Finally, a regression of nuisance covariates and their temporal derivatives (6 parameters derived from the rigid-body head motion correction, the signal averaged over the whole brain, the signal averaged over a region within the deep white matter, and the signal averaged from the ventricular CSF) was performed to remove spurious or regionally nonspecific signal variance.

To estimate the effects of susceptibility artifacts in the present data, the signal-to-noise (SNR) of the motion-corrected fMRI time series was computed for each voxel in the subject's native volumetric space by averaging the signal intensity across the whole run and dividing it by the standard deviation over time. The SNR was averaged across runs within subject when multiple runs were available. The SNR was then averaged across the 172 subjects. All areas in the TP exceeded the temporal SNR of 40 (Supplementary Fig. 1), which is considered to be the minimum to reliably detect effects between conditions in fMRI data (Murphy et al. 2007).

Seed Placement and Exploratory Functional Connectivity Analysis

Our first goal was to exhaustively explore the topography of functional connectivity using seeds that would provide an unbiased systematic sampling of the TP. For this purpose, we used whole-brain seed-based RSFC analysis in all participants. Forty seed regions of interest (ROIs) were manually placed encircling the anterior-to-posterior axis of the TP in standard MNI-152 stereotaxic space. The seed regions were spheres (2 mm radius) equidistant from each other and located in coronal planes separated anteroposteriorly 4 mm from each other, spanning from the tip of the temporal lobe to the limen insulae (fronto-temporal junction). The seeds covered the entire surface of the TP as shown in Figure 1. Table 2 lists the coordinates of each seed.

Correlation maps for each seed in the left TP were generated by computing the Pearson's product moment correlation "*r*" between the mean time course signal from each seed ROI (averaged over all voxels within each 2-mm-radius sphere) and every voxel in the brain. Positive correlation maps were then converted to *z*-maps using Fisher's *r*-to-*z* transformation. This transformation generates values for each voxel that are approximately normally distributed across individuals in a homogenous population. We chose a liberal threshold ($z > 0.04$) that is commonly used in functional connectivity studies because it provides results using seed-region methodology which are similar to the results obtained using independent component analysis (Van Dijk et al. 2010).

To test the reproducibility of our results across different samples, we first obtained separate connectivity maps for Dataset 1 ($n = 89$) and Dataset 2 ($n = 83$). We then calculated an η^2 coefficient for every seed pair between the 2 datasets to compute the similarity between the whole-brain RSFC map generated from a given seed in Dataset 1 with respect to the map generated from the same seed in Dataset 2. For more information on η^2 in RSFC, see Cohen et al. (2008). After the reliability of the connectivity maps was demonstrated using the η^2 coefficient and by visual inspection, we pooled all the subjects into a single-large sample ($n = 172$) to obtain the best estimate of the connectivity maps, which are reported in the Results section.

Cluster Analysis of Connectional Topography from Each of the 40 Seeds

Based on nonhuman primate tract-tracing data, several authors have proposed connectionally based subdivisions of the TP (Moran et al. 1987; Kondo et al. 2003). The goal of our cluster analysis was to try to establish, using an unbiased data-driven approach, the different large-scale systems anchored by subregions within the human TP. Clustering algorithms have been applied to RSFC data to try to parcellate brain regions, such as Broca's area (Kelly et al. 2010) and the precuneus (Margulies et al. 2009), into subregions based on similarities and differences in functional connectivity patterns with the rest of the brain.

To determine the various large-scale systems anchored within the TP, we performed a hierarchical clustering analysis in which subregions were grouped based on similarity of whole-brain functional connectivity topography. The degree of similarity was calculated using η^2 (as described in Cohen et al. 2008) across the z-transformed group-level RSFC maps of each seed region. An average-linkage hierarchical clustering analysis was performed on the pairwise η^2 matrix (40×40) using the Statistics Toolbox in MatLab (The Mathworks, Natick, MA, USA).

Temporal Pole Parcellation

To determine how the different functional subsystems identified using RSFC clustering analysis might relate to the cytoarchitectonic areas of the TP defined by Ding et al. (2009), we independently (blind to the results of the hierarchical clustering analysis) performed a parcellation of the TP following their cytoarchitectonic map. We manually traced regions of interest corresponding to cytoarchitectonic areas on the left TP of the standard MNI-152 T_1-weighted nonlinear 6th generation brain template brain (McConnell Brain Imaging Center, Montreal Neurological Institute, McGill University, Montreal; voxel size = $2 \times 2 \times 2$ mm), to which the T_1-weighted images had been previously co-registered. This procedure was performed after the original seeds had been placed and their connectivity determined, but before the hierarchical clustering analysis was performed.

The parcellation protocol was developed using the standard MNI-152 T_1-weighted template brain. We carried out the TP parcellation on the 6 successive rostrocaudal coronal sections used to place the seeds, spanning from the tip of the TP rostrally to the limen insulae caudally, reaching caudally the level where the temporal lobe merges with the frontal lobe (Fig. 1). In our protocol, Ding's area TG occupies the entire tip of the TP and extends posteriorly until the superior temporal sulcus (STS) appears on a coronal section (Fig. 1*C*). When the STS appears, TG recedes and anterior area TA starts. For the purpose of this study, anterior area TA includes Ding's areas TAr and TAp. We made this decision because the cytoarchitectonic structure of both areas is similar and because TAp is too small to be reliably localized on MRI. Anterior area TA occupies the superior temporal gyrus and extends from a lateral boundary in the fundus of the STS to a medial boundary formed by a previously undescribed semicircular notch on the dorsomedial surface of the TP (Supplementary Figs 2 and 3). This notch is perpendicular to the polar sulcus, which is often duplicated but is single in the standard MNI-152 T_1-weighted template brain. This notch is not yet present in the coronal section with the most rostral extent of STS and, therefore, here the medial boundary of TA has to be projected anteriorly from the coronal section immediately caudal to it. Moving caudally (Fig. 1*D*), when the occipitotemporal sulcus begins on coronal sections, areas 36 and TE appear. Area 36 borders ventromedially with area TG, the boundary being the inferior polar sulcus, if it exists, or, if not, a point located about ~8 mm medial to the single polar sulcus. Ventrolaterally area 36 borders with area TE and the boundary is the occipitotemporal sulcus. Area TE merges ventromedially with area 36 and dorsolaterally with anterior area TA. Proceeding caudally (Fig. 1*E*), the next section contains the most rostral portion of the parahippocampal gyrus; anterior area 35 and TI appear, TG disappears and area 36 recedes. Area TI, on the dorsomedial surface, extends from the edge of the semicircular temporal notch to the medial bank of the polar sulcus. Anterior area 35 borders dorsally on area TI and ventrally on area 36. The limit between area 35 and 36 at this level is determined by projecting rostrally the location of the rhinal sulcus, which appears in the coronal section immediately caudal to it (Fig. 1*F*). In this section, anterior entorhinal cortex (EC) begins and area 35 occupies the banks of the rhinal sulcus. Ding et al. (2009) describe anterior EC as one of the areas adjoining the TP, but do not list it among the TP areas. We describe the RSFC of anterior EC because it is included in the last coronal slice (see Fig. 1*F*) where the TP merges with the limen insulae. Anterior EC borders dorsally on the limen insulae and ventrally on area 35 at the dorsal bank of the rhinal sulcus. Area 35 extends from the border of the dorsal bank to the border of the ventral bank of the rhinal sulcus, and merges dorsally with rostral EC and ventrally with area 36. Area PI also appears in the most caudal coronal slice of our parcellation (seed 31 would correspond to PI); however, we include PI in TI because of its small size and the cytoarchitectonic similarity with TI.

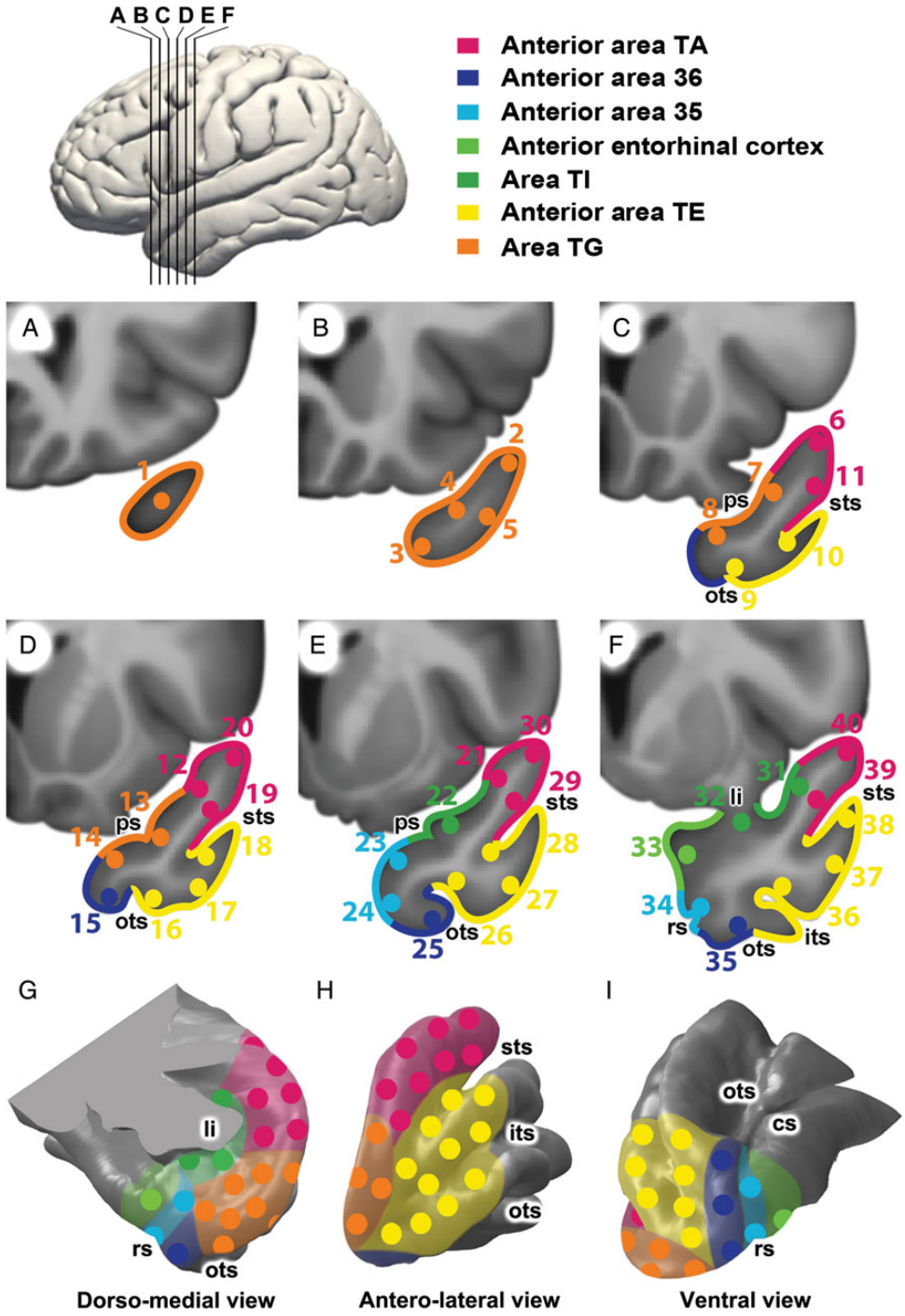

Figure 1. Placement of the 40 seed regions and parcellation of the left human TP on coronal sections of the TP (*A–F*) at the levels indicated on the lateral brain view at the top, and on surface views of the TP (*G–I*). Seed coordinates in MNI152 coordinate space are listed in Table 2. As described in the Materials and Methods section, seed placement was performed first, independent of a subsequent parcellation into likely cytoarchitectonic areas, listed at the top and color-coded. cs, collateral sulcus; its, inferior temporal sulcus; ps, polar sulcus; sts, superior temporal sulcus; ots, occipitotemporal sulcus; rs, rhinal sulcus; li, limen insulae.

To test the reliability of this protocol, an investigator (B.P.) traced manually the areas corresponding to the cytoarchitectonic areas and repeated the tracing 1 week later (retest). Additionally, we asked the first author of the cytoarchitectonic paper (Ding et al. 2009), S.L.D., to perform independently on the same MRI template the parcellation according to his previous description of the cytoarchitectonic areas. To test the similarity of the test–retest and interobserver parcellations, for each of the 7 areas (TG, anterior area TA, anterior area TE, anterior area 36, anterior area 35, TI, and anterior EC) and for the entire TP, we calculated the Dice coefficient, a metric that is defined as the number of voxels overlapping between 2 tracings divided by the mean number of voxels in the 2 tracings: Dice $(A,B) = 2\,|A$ and $B|/(|A|+|B|)$ where A and B are 2 segmentations performed by 2 different raters (Dice 1945). This measure determines whether both operators were demarcating the same voxels regardless of the size of the structure. This measure can also be applied to 2 tracings performed by the same operator to evaluate test–retest reliability. We followed the evaluative criteria set forth by (Landis and Koch 1977), in which agreement

Table 2
Location in MNI space for each of the 40 seeds used in the functional connectivity analysis

	Voxel location				Voxel location		
	x	*y*	*z*		*x*	*y*	*z*
Seed 1	−38	24	−32	Seed 21	−48	8	−12
Seed 2	−46	20	−22	Seed 22	−38	8	−24
Seed 3	−32	20	−38	Seed 23	−26	8	−32
Seed 4	−38	20	−30	Seed 24	−22	8	−42
Seed 5	−44	20	−32	Seed 25	−30	8	−44
Seed 6	−50	16	−14	Seed 26	−38	8	−38
Seed 7	−40	16	−24	Seed 27	−50	8	−40
Seed 8	−28	16	−34	Seed 28	−46	8	−28
Seed 9	−32	16	−42	Seed 29	−52	8	−18
Seed 10	−42	16	−36	Seed 30	−56	8	−6
Seed 11	−50	16	−22	Seed 31	−46	4	−14
Seed 12	−44	12	−20	Seed 32	−36	4	−24
Seed 13	−36	12	−28	Seed 33	−24	4	−30
Seed 14	−26	12	−32	Seed 34	−24	4	−42
Seed 15	−26	12	−42	Seed 35	−34	4	−44
Seed 16	−38	12	−42	Seed 36	−42	4	−40
Seed 17	−46	12	−38	Seed 37	−56	4	−32
Seed 18	−44	12	−30	Seed 38	−58	4	−22
Seed 19	−52	12	−22	Seed 39	−52	4	−18
Seed 20	−52	12	−10	Seed 40	−58	4	−4

Table 3
TP parcellation reliability

TP regions	Dice's overlap coefficient (%)	
	Test/re-test	Interobserver
Anterior area TA	91.93	92.19
Anterior area 36	90.07	84.25
Anterior area 35	94.81	76.44
Anterior EC	94.21	94.11
Area TI	95.30	94.53
Anterior area TE	91.06	92.93
Area TG	91.73	91.94
Entire TP	91.98	90.98

measures of correlation of 0.81–1.00 are "almost perfect," 0.61–0.80 are "substantial," and 0.41–0.60 are "moderate."

Once the cytoarchitectonic parcellation of the TP was done, we determined the correspondence between the different subsystems identified by the RSFC clustering analysis described above and the cytoarchitectonic regions by calculating the percentage of seeds located in each cytoarchitectonic region that were assigned to the same cluster. The networks described in the Results section were defined by the cluster analysis and its concordance with the cytoarchitectonic regions of the TP. To describe the connectivity of each network, we selected a representative seed in each cytoarchitectonic region, so long as the selected seed reflected the connectivity pattern of all the seeds in that region. If there were differences across seeds, we selected several seeds. This was only the case with anterior area TA, where anterior and posterior seeds had different connectivity patterns.

Review of Tract-Tracing Literature in Nonhuman Primates

Finally, to relate our findings in humans with data from tract-tracing studies in nonhuman primates, we used PubMed to retrieve all the references to TP connectivity in monkey and reviewed in addition all the relevant publications cited in the articles retrieved.

Results

Functional Connectivity of the TP in Humans

TP RSFC was very similar in the 2 independent datasets studied (Supplementary Fig. 4). Similarity coefficients (η^2) exceeded 0.7 for all 40 seeds and 0.8 for 27 of the 40 seeds. Cortical RSFC correlation maps (for the entire sample, including both datasets) for each of the 40 seeds are provided in Supplementary Table 2 and Supplementary Fig. 5.

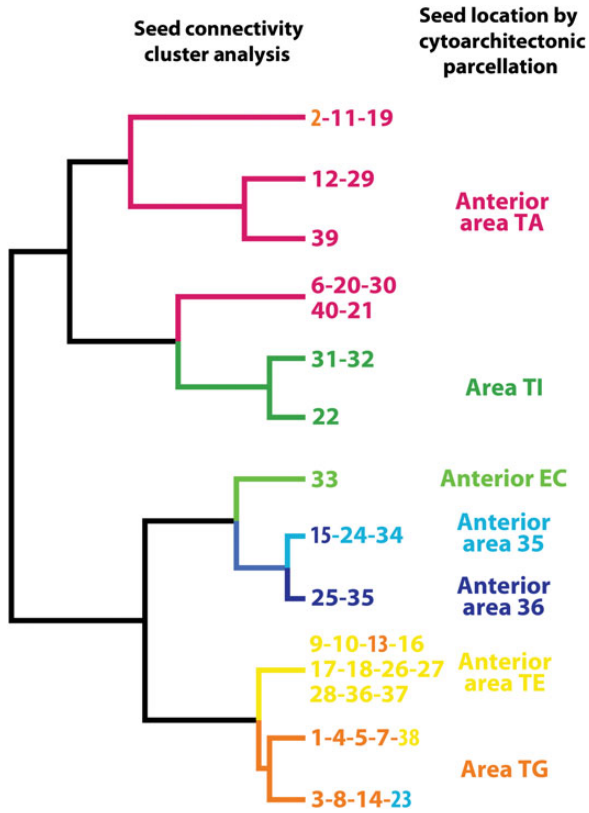

Figure 2. Seed clusters resulting from the functional connectivity hierarchical clustering analysis (left) and areas defined by the independently performed anatomic TP parcellation corresponding to the cytoarchitectonic areas described by (Ding et al. 2009) (right). Seed ROI numbers are color-coded to correspond to the anatomic subregion in which the seed was located. Note the striking correspondence between the 2 independent classification methods. Only 5 seeds were located in a discordant cluster. Three of these (seeds 13, 15, 38) were located in the concordant superior cluster.

The manual parcellation of the TP on the MRI outlined the 7 subregions shown in Figure 1, corresponding to the cytoarchitectonic subregions described histologically by Ding et al. (2009). Test–retest and inter-rater reliability (between B.P. and S.L.D.) for the parcellation of the TP in the standard T_1 brain MRI were high (Table 3). The average Dice coefficient across all subregions was 93% for test–retest and 90% for inter-rater reliability.

The cluster analysis of TP RSFC, conducted to explore potential functional subdivisions of the TP based on its connectivity, yielded the tree shown in Figure 2. The first level yielded 2 distinct systems. One included the dorsal TP: anterior area TA and TI. The other included the ventral TP, which could be subdivided into 2 subsystems: anterolateral, including TG and anterior area TE, and ventromedial, including anterior area 35, anterior area 36, and anterior EC.

Strikingly, for 87.5% of the seeds, seed grouping by the hierarchical cluster analysis corresponded to seed location in the independently performed cytoarchitectonic parcellation of the TP (Figs 1 and 2). Only 5 seeds were allocated by the cluster analysis to a discordant cluster. Of these 5, 3 seeds (13, 15, and 38) were appropriately located in terms of the immediately superior level (Fig. 2).

Given the concordance between the anatomical and functional connectivity data, we will summarize the RSFC for the 40 seeds by describing the connectivity of representative seeds corresponding to each cytoarchitectonic area. The seeds we describe in detail are also those for which the RSFC was most concordant between the 2 independent datasets studied (Supplementary Fig. 4). The results of our extensive review of TP tract-tracing connectivity in the monkey are listed in Supplementary Table 2 and are discussed in the last Results subsection. Based on a combination of their functional connectivity, their locations with respect to cytoarchitectonic subregions, and the clustering analysis, we grouped the areas into 4 regions.

Dorsal Region (Somatosensory–Auditory)

Anterior area TA. This is a relatively large area, located in the dorsal TP, immediately posterior to area TG, which is in the tip of the TP (Fig. 1). In anterior area TA, functional connectivity clearly distinguished 2 subregions: one more posterior, represented by seed 40, and one more anterior, represented by seed 6 (Figs 3 and 4, somatosensory–auditory network). Seed 40 had bilateral RSFC with peri-Rolandic cortex: both precentral and postcentral gyri on the lateral aspect of the hemisphere and to a lesser extent with the paracentral lobule in the medial aspect of the hemisphere (Figs 3 and 4, seed 40, lateral and medial views). In addition to primary somatosensory/motor cortex, primary auditory cortex (Fig. 5, seed 40, Heschl's gyrus) and primary olfactory cortex (Fig. 5, seed 40, piriform cortex) also had strong RSFC with seed 40. In the medial frontal lobe, the most prominent RSFC was with the supplementary motor area and the middle portion of the cingulate gyrus (Figs 3 and 4, seed 40, medial view), generally considered to be the motor section of the cingulate cortex. Strong bilateral RSFC was present with the entire insula; this was the only seed with connectivity to the entire insula, encompassing both its anterior and posterior portions (Figs 3–5, seed 40, striatum levels). Within the TP, seed 40 was connected to area TG, but not to basal areas. Among subcortical structures, seed 40 had unilateral RSFC with a portion of the caudate tail in the paracentral region, but bilateral RSFC with the rostrodorsal and medial amygdala, posterior putamen and claustrum, as well as with the ventrolateral and centromedian nuclei of the thalamus (Fig. 5, seed 40). Both of these thalamic nuclei are critical in sensorimotor integration; the centromedian nucleus projects to striatum and the ventrolateral nucleus projects to BA 4 in the precentral gyrus. There was no connectivity with the brain stem (Fig. 6) but, in the cerebellum, there was bilateral RSFC with the paravermian portion of hemispheric lobes VI and VIIB (Schmahmann et al. 1999), both involved in the coordination of sensorimotor activity (Stoodley and Schmahmann 2010) (Fig. 7, seed 40). In summary, the connectivity of seed 40 suggests an important role for this posterior portion of anterior area TA in the integration of auditory and somatosensory information, at the level of primary sensorimotor cortical areas and anatomically related subcortical regions.

Rather than with primary auditory and somatosensory cortices, seed 6 exhibited RSFC with adjacent secondary unimodal cortices for the same modalities (Figs 3 and 4). In contrast to seed 40, there was no RSFC with Heschl's gyrus but rather with adjacent auditory cortex on the superior temporal gyrus surrounding Heschl's gyrus (Fig. 5, seed 6, Heschl's gyrus). Likewise, seed 6 had RSFC with association cortex caudal (parietal) and rostral (frontal) to peri-Rolandic primary cortex, and predominantly with its ventral portion, which largely subserves mouth and tongue movement (Figs 3 and 4, seed 6, lateral view). Most notably, seed 6 exhibited RSFC with all major nodes of the large-scale language network (inferior and middle frontal gyri, supramarginal gyrus, superior, and mid-to-caudal middle temporal gyri (Hickok and Poeppel 2007) with a prominently left-lateralized pattern (compare Figs 3 and 4, seed 6). The caudal area within the temporal lobe extending from superior temporal gyrus down into STS and middle temporal gyrus includes a key region implicated in lexical retrieval (Damasio et al. 1996). Connectivity with the right hemisphere included a homologous region within the STS implicated in the ability to selectively identify a sound of interest from a background of competing sounds (Teki et al. 2011; Fig. 4, seed 6). Seed 6 exhibited also RSFC with the central and lateral parts of the orbitofrontal cortex (Figs 3 and 4, seed 6, ventral view). In the medial aspect of the hemisphere (Figs 3 and 4, seed 6, medial view), RSFC was present with SMA as with seed 40, but more so with preSMA and neighboring frontal and cingulate cortex, in regions more rostral than those connected to seed 40. Rather than the entire insula, as for seed 40, only the anterior insula had bilateral RSFC with seed 6 (Fig. 5, dorsal striatal level). RSFC with the TP had a similar topography as for seed 40, including mainly area TG, but was more extensive than for seed 40. As with seed 40, seed 6 connected to the rostro-dorsal and medial amygdala but not to hippocampus (Figs 3 and 4, seed 6, medial view, and Fig. 5, seed 6, amygdala). RSFC with other subcortical structures showed a network functionally related to association cortex: the dorsal portion of the head and anterior portion of the body of the caudate nucleus, a rostrodorsal portion of the putamen and ventral-anterior and centromedian nuclei of the thalamus: all with ipsilateral predominance (Fig. 5, seed 6). However, there was also RSFC with subcortical limbic structures, such as the ventromedial portion of the caudate heads, medial globus pallidus, and premammillary hypothalamus, all of them with much more symmetrical connectivity, as well as more ipsilaterally with dorsomedial and anterior nuclei of the thalamus (Fig. 5, seed 6). In the cerebellum, seed 6 had contralateral RSFC with the posterior aspect of Crus I and II (lobule VII), a region mediating language and other cognitive abilities (Stoodley and Schmahmann 2010; Stoodley et al. 2010) (Fig. 7, seed 6).

In summary, the cortex on the most rostral portion of the dorsal TP tapped by seed 6 had preferentially ipsilateral (left-hemispheric) connectivity with association cortex typically considered to compose the large-scale language network and association auditory cortices, in stark contrast with seed 40, which was connected bilaterally to primary cortex of the same modalities. Seed 6 was also connected with subcortical structures related to higher order sensorimotor processing and limbic integration, such as the ventral-anterior, dorsomedial, and anterior thalamic nuclei.

Ventromedial Region (Visual)

Anterior area 36. Anterior area 36, represented by seed 25, was identified as the anterior extent of Brodmann area 36, located on the medial bank of the collateral sulcus (Fig. 1). Anterior area 36, together with anterior area 35, belongs to perirhinal cortex. Anterior area 36 showed strong bilateral RSFC with the most rostral areas of the occipitotemporal visual

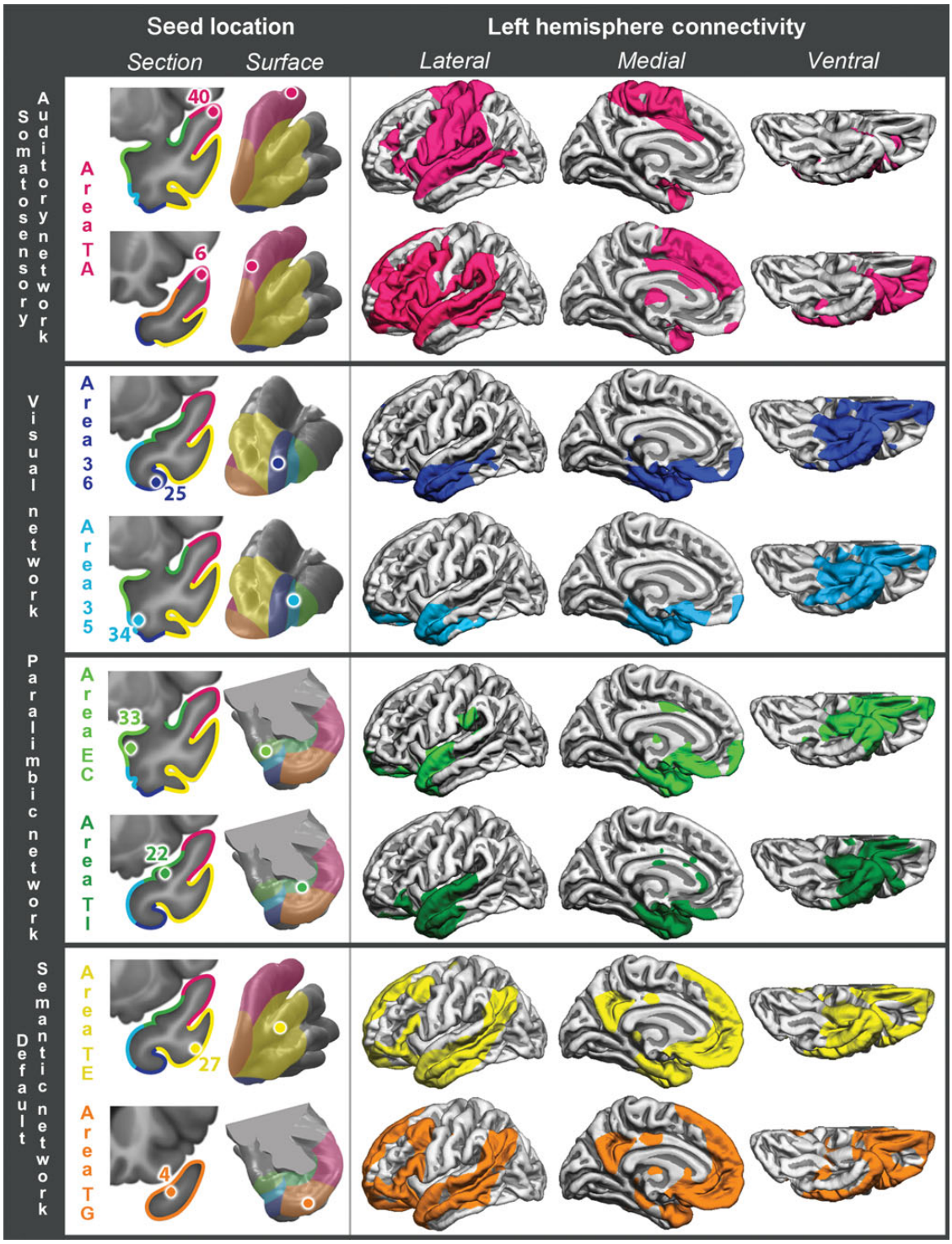

Figure 3. Left hemisphere cortical RSFC for 8 representative seeds, listed and illustrated in the left column of images. They are grouped into 4 large-scale networks by both anatomical and functional criteria, as discussed in the text.

system, including the anterior portion of the fusiform gyrus, inferior and middle temporal gyri, anterior hippocampal formation, and EC (Figs 3 and 4, seed 25, lateral, medial, and ventral views). Prominent connectivity was present with other areas in the ventral and rostral TP, including TE and TG. There was also extensive RSFC with orbitofrontal cortex, extending to medial prefrontal cortex and anterior insula (Figs 3–5). While there was connectivity with the olfactory tubercle, there was none with piriform cortex, a primary olfactory area. Among subcortical structures, seed 25 was connected bilaterally with the basolateral amygdala, medial and lateral basal forebrain, the nucleus accumbens, the globus pallidus medialis (mostly ipsilateral), and with the hypothalamus (Fig. 5, seed 25). Finally, area 36 showed strong connectivity

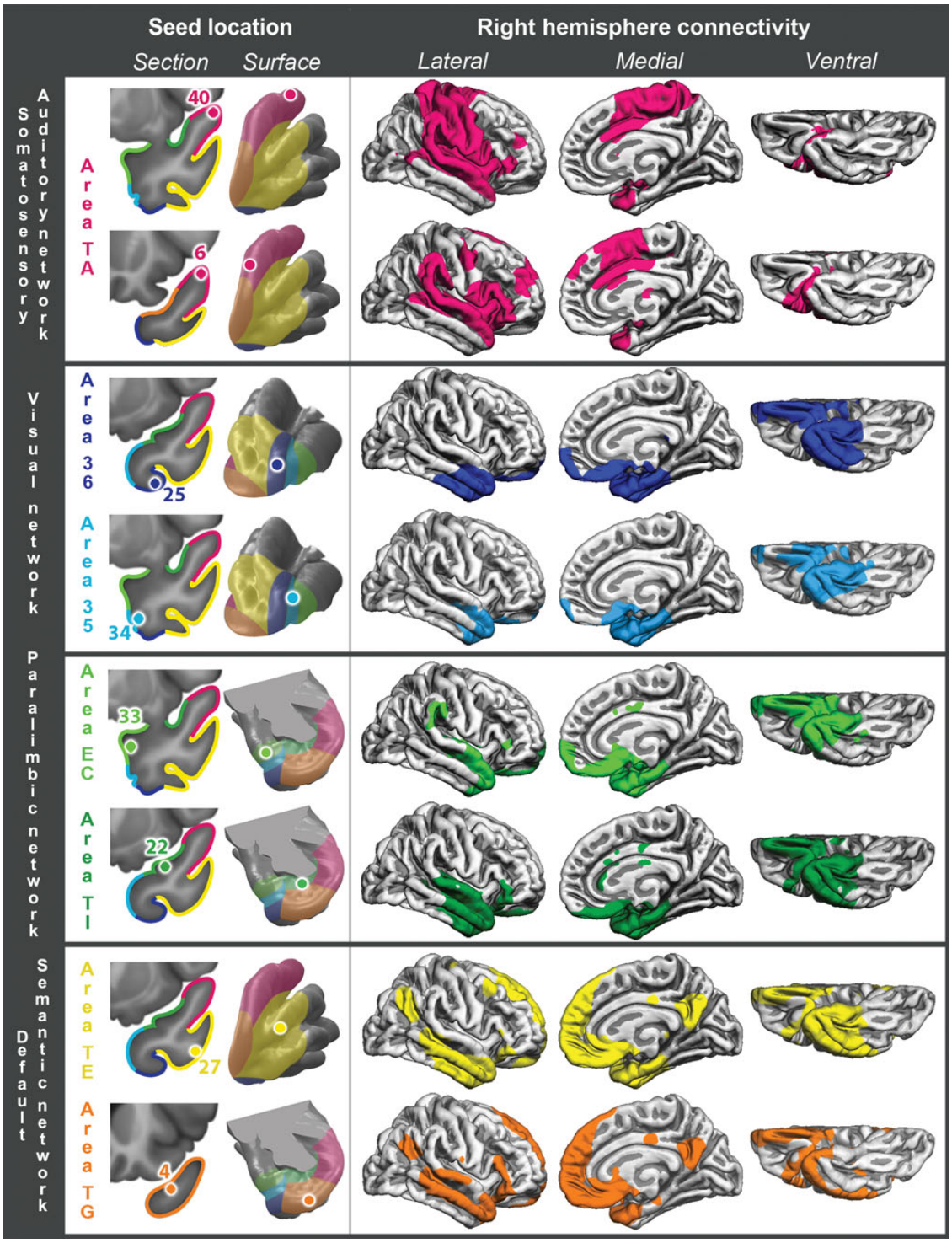

Figure 4. Right hemisphere cortical RSFC for 8 representative seeds, listed in the left column. Left and right RSFC patterns were generally quite symmetrical, with the notable exception of seed 6 on anterior area TA, which had preferentially ipsilateral (left-hemispheric) connectivity with perisylvian association cortex, typically considered to encompass the large-scale language network and association auditory cortices.

with the brainstem, mainly with the ventral tegmental area of the midbrain, pons, basis pontis, and tegmentum (vestibular nuclei), and medullary tegmentum (Fig. 6, seed 25), as well as with the most anterior portion of the cerebellar vermis and Schmahmann's lobule V bilaterally, but more extensive ipsilaterally (Fig. 7, seed 25).

Anterior area 35. Anterior area 35, represented by seed 34, is a small area localized rostral to the most rostral portion of the EC, in the fundus and the lateral bank of the rhinal sulcus (Fig. 1). The pattern of RSFC of this region resembled that of anterior area 36, showing strong connectivity with rostral visual association areas (Figs 3 and 4, seed 34, lateral, medial,

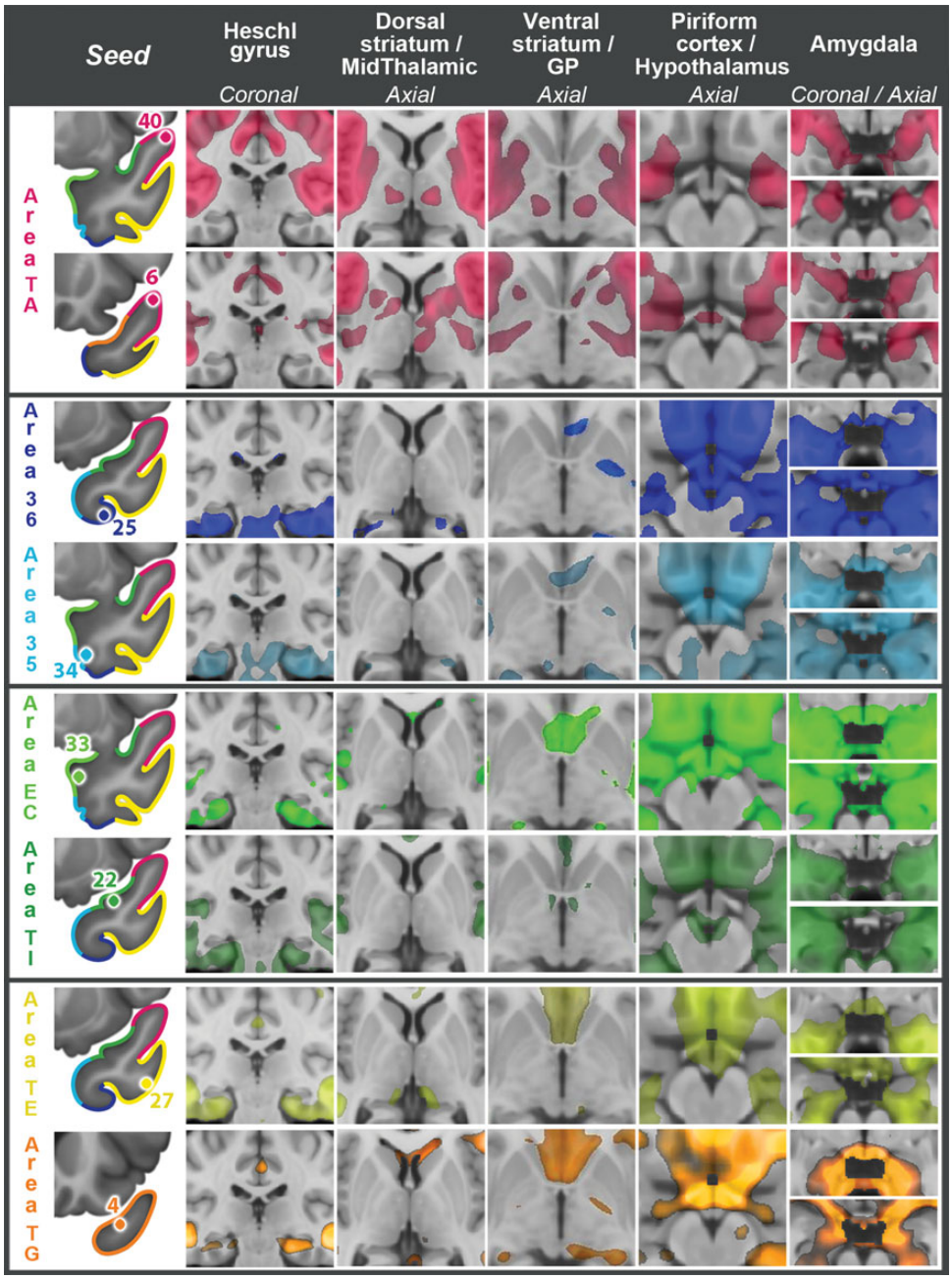

Figure 5. Bilateral RSFC with Heschl's gyrus and multiple subcortical structures for 8 representative TP seeds, listed in the left column. Images follow the radiological orientation (left side of the brain is on the right side of the image). GP, globus pallidus.

and ventral views) and greater connectivity than area 36 with the posterior hippocampus and parahippocampal cortex (Supplementary Fig. 5). Connectivity with the amygdala was even more extensive than for area 36, involving bilaterally most of the amygdala (Fig. 5, seed 34, amygdala). Area 35 was less extensively connected than 36 with orbitofrontal cortex, mostly medial, extending minimally to medial prefrontal cortex (Figs 3 and 4, seed 34, medial and ventral views). It was also bilaterally connected to 2 small portions of the insula, one rostroventral and another dorsal. It had no connectivity with the piriform cortex. Unlike area 36, area 35 showed no connectivity with the forebrain or ventral tegmental area. It connected with the anterior hypothalamus, but not with the mammillary bodies (Fig. 5, seed 34, hypothalamus). In the brainstem, anterior area 35 showed RSFC with a large bilateral cluster in ponto-mesencephalic tegmentum, including the region of the locus coeruleus bilaterally (Fig. 6, seed 34). It had RSFC with the basis pontis, extending into the medullary tegmentum (Fig. 6, seed 34). Like area 36, area 35 connected bilaterally to vestibular nuclei, but to lateral, rather than superior, vestibular nucleus. In the cerebellum, it had bilateral RSFC with Schmahmann's lobule V bilaterally, reaching, but not including, the most anterior vermis (Fig. 7, seed 34).

In summary, the perirhinal region of the TP, rostral areas 36 and 35, exhibited preferential RSFC with the most rostral unimodal visual areas of the ventral or occipitotemporal

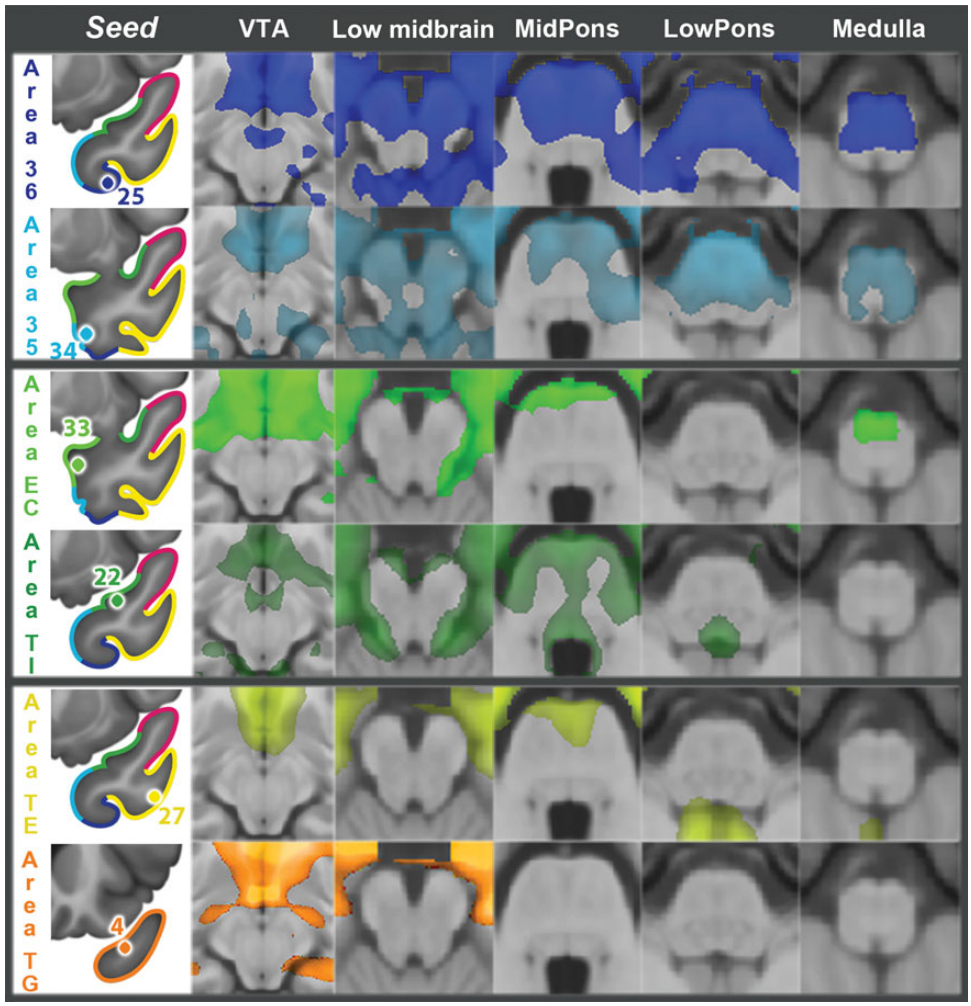

Figure 6. RSFC with brainstem for 8 representative TP seeds, listed in the left column. The headings refer to brainstem regions or to representative structures at the level of the section. Images follow the radiological orientation (left side of the brain is on the right side of the image). VTA, ventral tegmental area.

pathway, and also strong connectivity with paralimbic cortical and limbic subcortical regions as well as the brainstem and cerebellum.

Medial Region (Paralimbic)

Anterior EC. This region, represented by seed 33, is the most rostral part of the EC, medial to Brodmann's area 35 (Fig. 1). As with other areas in the ventromedial aspect of the TP, anterior EC showed remarkably symmetrical bilateral connectivity, mostly with structures in the anterior temporal region, including the entire amygdala, orbitofrontal cortex, nucleus accumbens, and hypothalamus (Figs 3–5, seed 33). It had strong RSFC with the rest of the EC and with the anterior hippocampal formation, including the anterior fourth of the dentate gyrus, as well as with perirhinal and parahippocampal cortices (Fig. 2, seed 33, medial view). The area of connectivity extended slightly more caudally on the ipsilateral side. It also extended caudally along the fusiform gyrus, tapering caudally to include the lips of the inferior temporal sulcus (Figs 3 and 4, seed 33, ventral view). Rostral EC had RSFC with olfactory cortex in the olfactory tubercle, located at the caudal extent of the gyrus rectus, and with the piriform cortex, but the connectivity was not as extensive as for area TI, described immediately below. Rostral EC was connected with all other areas of the temporal tip, except a lateral portion of TE. On the superior temporal cortex, this area of connectivity extended as far back as the anterior margin of Heschl's gyrus, but did not include primary auditory cortex (Figs 3 and 4, seed 33, lateral view and Fig. 5). The area of superior temporal gyrus connectivity extended ventromedially into the bed of the Sylvian fissure, ascending on the opposite bank to include the ventral half of the insular cortex. In addition to the orbitofrontal connectivity, in frontal lobe EC showed RSFC with the frontal pole and with a small area of paracentral cingulate cortex (Figs 3 and 4, seed 33, medial view). Among subcortical regions, rostral EC showed bilateral RSFC with nucleus accumbens, the medial and lateral forebrain, and with the entire hypothalamus (Fig. 5, seed 33), as well as with the arcuate nucleus on the ventral surface of the medulla (Fig. 6, seed 33). No RSFC was observed with the cerebellum.

Area TI. The temporal insular cortex (TI) is a small area, located in the posterior portion of the TP, which merges posteriorly with the limen insulae, and was represented by seed 22 (Fig. 1). In its connectivity it resembled EC but with some important differences. TI exhibited extensive bilateral

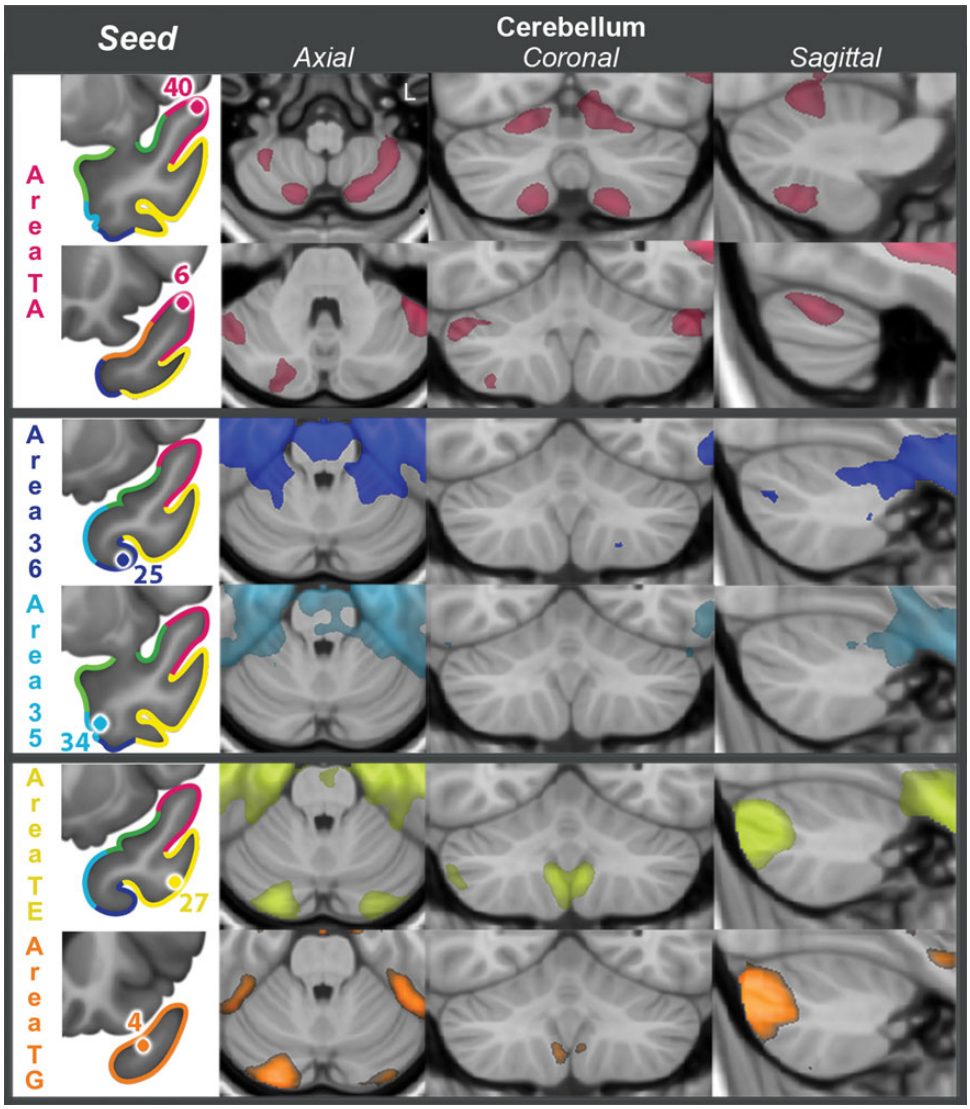

Figure 7. RSFC with cerebellum for 6 representative TP seeds, listed in the left column. Images follow the radiological orientation (left side of the brain is on the right side of the image).

RSFC with primary olfactory cortex on olfactory tubercle and piriform and periamygdaloid cortex (Fig. 5, seed 22, Heschl's gyrus and piriform), as well as with amygdala, EC, hippocampal head, rostral parahippocampal gyrus, orbitofrontal cortex, and anterior cingulate gyrus (Figs 3 and 4, seed 22, medial view). As regards the TP, RSFC was remarkably absent with most of areas TG and TE, on the tip and lateral aspect of the TP, respectively. Like EC, it had RSFC with the superior temporal gyrus, but including Heschl's gyrus for TI (Fig. 5), and with the inferior portion of insular cortex, in continuity with the superior aspect of the superior temporal gyrus (Figs 3 and 4, seed 22, lateral view). RSFC was also present with nucleus accumbens and lateral portions of the basal forebrain (Fig. 6, seed 22). Unlike EC, it had no RSFC with medial hypothalamus, but instead, it had bilateral RSFC with the bed nucleus of the stria terminalis (Supplementary Fig. 6), VTA, and symmetrical regions of the pontine tegmentum, including the medial raphe and the region of the locus coeruleus (Fig. 6, seed 22).

In summary, rostral EC and TI exhibited strong connectivity to olfactory cortex, sharing extensive bilateral connections to anterior temporal structures and orbitofrontal cortex. Both regions showed extensive connectivity with the amygdala and the hypothalamus. EC was connected to the arcuate nucleus of the medulla and TI, by contrast, to the bed nucleus of the stria terminalis, VTA, medial raphe nucleus, and the region of the locus coeruleus.

Anterolateral Region (Default-Semantic Network)

Anterior area TE. Temporal area TE extends along the middle and inferior temporal gyri, ventral to anterior area TA and caudal to area TG. Anterior area TE was represented by seed 27 (Fig. 1). It had strong bilateral RSFC with default network areas, including the medial prefrontal cortex (both ventromedial and dorsomedial), precuneus and posterior cingulate cortex, heteromodal posterior inferior parietal lobe (especially temporoparietal junction and the angular gyrus), dorsolateral prefrontal cortex, middle temporal gyrus, and the parahippocampal gyrus (Figs 3 and 4, seed 27, lateral and medial view). But, in addition to the default network connectivity, this seed also showed strong connectivity with

other cortical areas not typically thought of as part of the default network, including orbitofrontal and ventrolateral prefrontal cortex, as well as anterior inferior temporal gyrus. In fact, its connectivity is probably more similar to the so-called semantic network, which to a great extent overlaps with the default network but is not identical to it (Binder et al. 2009). TE was connected with lateral, ventral, and anterior regions on the TP, including area TG, but not with the most posterior dorsal portion of the TP. It was connected to the caudoventral amygdala (Fig. 5, seed 27) and the hippocampal formation (Figs 3 and 4, seed 27, medial and ventral view). Similar to area 35, area TE exhibited no connectivity with deep gray nuclei, other than a small, medial portion of the pulvinar (Fig. 5, seed 27). However, it was connected to the hypothalamus (Fig. 5, seed 27). In the brain stem, there was connectivity with the pontine nuclei, more pronounced ipsilaterally, and with a region in the contralateral pontine tegmentum (Fig. 6, seed 27). In the cerebellum, there was bilateral RSFC with Crus I and II, in the posterior portion of the cerebellar hemispheres, and with the medial aspect of the cerebellar tonsils. In both cases the region connected was slightly larger on the contralateral hemisphere (Fig. 7, seed 27).

Area TG. Area TG, represented by seed 4, occupies the tip of the TP and the anterior portion of its dorsomedial aspect (Fig. 1). Similar to seed 27, seed 4 exhibited strong RSFC with default-semantic network areas, including the medial prefrontal cortex, precuneus and posterior cingulate cortex, temporoparietal junction, dorsolateral prefrontal cortex, middle temporal gyrus, and parahippocampal gyrus (Figs 3 and 4, seed 4, lateral and medial view). Seed 4 also showed strong connectivity with areas along the medial edge and caudolateral orbitofrontal cortex, and with regions in the ventrolateral prefrontal cortex. In general, the connectivity of this region was more lateralized to the ipsilateral side than for areas in the ventral and ventromedial aspect of the TP, or even TE. This was true not only for the dorsolateral prefrontal cortex, with only unilateral connectivity, but also for the orbitofrontal, medial temporal, and inferior parietal clusters as well (Figs 3 and 4, seed 4, lateral and medial view). TG showed RSFC with all other areas of the TP, except with area TI. Among other temporal lobe structures, TG was connected bilaterally to medial amygdala (Fig. 5, seed 4) and to the hippocampal formation (Figs 3 and 4, seed 4, medial and ventral view). Here, connectivity extended anteroposteriorly including the head of the hippocampus and neighboring entorhinal and perirhinal cortex, and with the midportion of the fusiform gyrus (Figs 3 and 4, seed 4, ventral view). TG showed RSFC with the cortex in the STS, extending from the TP to the angular gyrus, but was not connected to olfactory cortex. Subcortical connectivity was bilateral and included nucleus accumbens, the septal nuclei, and the anterior hypothalamus, excluding the mammillary bodies (Fig. 5, seed 4). In the cerebellum, there was RSFC with TG on the posterior aspect of Crus I of the cerebellar hemispheres and in the cerebellar tonsil (Fig. 7, seed 4). In both cases, the contralateral component was larger than the ipsilateral one, in agreement with the supratentorial finding of ipsilateral connectivity to the dorsolateral prefrontal cortex.

In summary, the RSFC of this region, anterior area TE and TG, is characterized by its strong connectivity to all regions of the default-semantic network and the limbic medial temporal regions, including the amygdala, hippocampus, and parahippocampal gyrus. TG in particular is connected to all other regions of the TP.

Review of Anatomic Connectivity Studies in Monkey

Using the macaque cytoarchitectonic nomenclature employed by Kondo et al. (2003) and Moran et al. (1987), we have listed in Table 4 all the extant publications containing descriptions of tract-tracing connectivity to and from the macaque TP. According to Ding et al. (2009)—although a detailed comparative study may be needed to compare the small TP of monkeys with the large TP of the humans—currently available cytoarchitectonic data suggest that the dysgranular and granular dorsal areas of the monkey TP (TGdd and TGdg) may correspond to area TG and anterior area TAr of the human TP, respectively. The medial agranular area of the monkey TP (TGa) appears to correspond to area TI in humans. In the ventral area of the monkey TP, the dysgranular area (TGvd) may correspond to anterior areas 35 and 36 of the human TP, and the granular area plus the lower portion of the STS (TGvg and lower TGsts) would correspond roughly to anterior area TE. Finally, the upper portion of the STS in the monkey TP (upper TGsts) appears to correspond to the small anterior area TAp in humans.

TGdg and Upper TGsts (Corresponding to Anterior Area TA)

Similar to human area TA, TGdg and upper TGsts in the macaque exhibits anatomical connectivity with primary auditory and olfactory cortices and with the association cortex of the same modalities: pyriform and anterior insular regions (Mesulam and Mufson 1982; Mufson and Mesulam 1982), and with the entire superior temporal gyrus (Galaburda and Pandya 1983; Seltzer and Pandya 1989, 1994). Nevertheless, there is no macaque anatomical tracing literature indicating connectivity between TGdg and primary motor or somatosensory cortex. Within the prefrontal cortex, clear interspecies differences are also noted for the medial and orbital regions. In humans, while anterior area TA was connected with the medial and lateral orbital surfaces, there was no RSFC with ventromedial prefrontal cortex (Figs 3 and 4, seed 6, lateral and ventral views). In monkeys, both ventromedial and orbital prefrontal regions are strongly connected with TGdg (Fig. 4 in Kondo et al. (2003)). However, anterior area TA in humans showed a connectivity pattern very similar to the tracer injection in the most rostral area of the STS in the macaque, which is strongly connected with the medial and lateral orbitofrontal cortex, not including areas along the medial edge of the orbital cortex or medial prefrontal regions (Fig. 5 in Kondo et al. (2003)). But tracing studies in macaque have not identified connectivity of TGdg with other portions of the medial frontal lobe, such as the supplementary motor area and the central portion of the cingulate gyrus, which in the human brain exhibited RSFC with anterior area TA. As in humans, connectivity with the ventrolateral prefrontal cortex has been described by anatomical tracing in the macaque (Petrides and Pandya 2002, Cases 1–3). Finally, the anatomical tracing literature shows connectivity of the dorsal TP with the thalamus, like in humans, but with different nuclei. In macaque, there is evidence for connectivity with geniculate bodies, pulvinar, and mediodorsal nuclei (Yeterian and Pandya 1989, 1991; Pandya et al. 1994), whereas, in humans, RSFC linked TA to thalamic regions likely representing nuclei related to primary and associative motor-somatosensory processing.

Table 4
Anatomical connectivity of the TP in macaque monkey

Connecting area	TGdd[a]	TGdg	TGsts	TGvg	TGvd	TGa
Frontal lobe						
Frontal pole	Kondo et al. (2003) (Fig. 10) Barbas et al. (1999) (Fig. 7)	Petrides and Pandya (2007) (Case 1) Kondo et al. (2003) (Fig. 4) Romanski et al. (1999) (Fig. 3) Barbas et al. (1999) (Fig. 7) Moran et al. (1987) (Fig. 3)	Petrides and Pandya (2007) (Case 1)		Moran et al. (1987) (Fig. 5)	Barbas et al. (1999) (Fig. 7)
Ventromedial prefrontal cortex	Saleem et al. (2008) (Figs 3 and 11) Kondo et al. (2003) (Figs 7 and 10) Barbas et al. (1999) (Figs 3, 4, and 8) Romanski et al. (1999) (Fig. 6) Barbas (1988) (Fig. 6) Moran et al. (1987) (Fig. 4)	Saleem et al. (2008) (Figs 3, 8, and 11) Schmahmann and Pandya (2006) (Case 11) Kondo et al. (2003) (Figs 4 and 7) Barbas et al. (1999) (Figs 3, 4, and 8) Romanski et al. (1999) (Fig. 6) Barbas (1988) (Fig. 6) Moran et al. (1987) (Cases 3 and 11)	Saleem et al. (2008) (Fig. 3) Kondo et al. (2003) (Fig. 8)	Saleem et al. (2008) (Fig. 3)	Saleem et al. (2008) (Fig. 3) Barbas et al. (1999) (Fig. 4) Barbas (1988) (Fig. 6) Moran et al. (1987) (Fig. 5)	Saleem et al. (2008) (Figs 3 and 11) Kondo et al. (2003) (Fig. 8) Romanski et al. (1999) (Fig. 6)
Orbitofrontal cortex	Saleem et al. (2008) (Fig. 3) Muñoz and Insausti (2005) (Fig. 5) Kondo et al. (2003) (Figs 7 and 10) Romanski et al. (1999) (Fig. 5) Barbas (1993) (Figs 5, 6, and 9) Barbas (1988) (Fig. 2) Moran et al. (1987) (Figs 4 and 9)	Saleem et al. (2008) (Fig. 9) Schmahmann and Pandya (2006) (Case 11) Muñoz and Insausti (2005) (Fig. 5) Kondo et al. (2003) (Figs 4 and 7) Barbas (1993) (Figs 5, 6, and 9) Romanski et al. (1999) (Fig. 5) Moran et al. (1987) (Figs 3 and 9) Barbas (1988) (Fig. 2)	Saleem et al. (2008) (Figs 3 and 9) Petrides and Pandya (2007) (Case 7) Muñoz and Insausti (2005) (Fig. 5) Kondo et al. (2003) (Figs 5 and 11) Barbas (1993) (Figs 6, 7, and 9) Barbas (1988) (Fig. 2) Moran et al. (1987) (Fig. 9)	Saleem et al. (2008) (Fig. 3) Petrides and Pandya (2007) (Case 7) Kondo et al. (2003) (Fig. 7) Barbas (1993) (Figs 6, 7, and 9) Barbas (1988) (Fig. 2) Moran et al. (1987) (Fig. 9)	Saleem et al. (2008) (Fig. 3) Muñoz and Insausti (2005) (Fig. 5) Kondo et al. (2003) (Fig. 7) Barbas (1993) (Figs 6, 7, and 9) Barbas (1988) (Fig. 2) Moran et al. (1987) (Figs 5 and 9)	Saleem et al. (2008) (Figs 3 and 9) Schmahmann and Pandya (2006) (Case 33) Muñoz and Insausti (2005) (Fig. 5) Romanski et al. (1999) (Figs 5 and 6) Barbas (1993) (Figs 6, 7, and 9) Barbas (1988) (Fig. 2) Moran et al. (1987) (Fig. 9)
Ventrolateral prefrontal cortex	Romanski et al. (1999) (Fig. 9) Barbas (1988) (Fig. 4)	Petrides and Pandya (2002) (Cases 1 and 2) Romanski et al. (1999) (Fig. 9) Barbas (1988) (Fig. 4)	Saleem et al. (2008) (Fig. 13) Kondo et al. (2003) (Figs 5and 11) Petrides and Pandya (2002) (Cases 2-4) Romanski et al. (1999) (Fig. 9) Barbas (1988) (Figs 3 and 4)	Saleem et al. (2008) (Fig. 13) Petrides and Pandya (2002) (Cases 2–5) Barbas (1988) (Figs 3 and 4)	Petrides and Pandya (2002) (Cases 3–5) Barbas (1988) (Fig. 4)	Romanski et al. (1999) (Fig. 9) Barbas (1988) (Fig. 4)
Dorsolateral prefrontal cortex	Barbas et al. (1999) (Fig. 6)	Petrides and Pandya (2007) (Case 4) Petrides and Pandya (1999) (Cases 4, 7, and 8) Romanski et al. (1999) (Figs 4 and 8) Barbas et al. (1999) (Fig. 6)	Petrides and Pandya (2002) (Case 4) Romanski et al. (1999) (Figs 4 and 8) Petrides and Pandya (1999) (Cases 4, 7, and 8)	Schmahmann and Pandya (2006) (Case 32)	Petrides and Pandya (1999) (Cases 4, 7, and 8) Moran et al. (1987) (Fig. 5)	
Cingulate						
Anterior cingulate	Muñoz and Insausti (2005) (Figs 3 and 4) Kondo et al. (2003) (Figs 7 and 10) Barbas et al. (1999) (Fig. 2) Barbas (1988) (Fig. 7) Moran et al. (1987) (Fig. 4) Morecraft and Van Hoesen (1998) (Cases 3, 18)	Petrides and Pandya (2007) (Case 6) Schmahmann and Pandya (2006) (Cases 11 and 23) Muñoz and Insausti (2005) (Figs 3 and 4) Kondo et al. (2003) (Figs 4 and 7) Barbas et al. (1999) (Fig. 2) Barbas (1988) (Fig. 7) Moran et al. (1987) (Figs 3 and 9)	Petrides and Pandya (2007) (Case 6) Kondo et al. (2003) (Fig. 5)		Moran et al. (1987) (Fig. 5)	
Insula						
Anterior insula	Saleem et al. (2008) (Fig. 9) Kondo et al. (2003) (Figs 7 and 10) Moran et al. (1987) (Fig. 4) Mesulan and Mufson (1982) (Fig. 1)	Saleem et al. (2008) (Fig. 9) Kondo et al. (2003) (Figs 4 and 7) Mesulan and Mufson (1982) (Fig. 1) Mufson and Mesulan (1982) (Fig. 5)	Saleem et al. (2008) (Fig. 9) Kondo et al. (2003) (Figs 5 and 11) Mesulan and Mufson (1982) (Fig. 1)	Saleem et al. (2008) (Fig. 9) Kondo et al. (2003) (Fig. 7) Mesulan and Mufson (1982) (Fig. 1) Mufson and Mesulan (1982) (Fig. 1)	Saleem et al. (2008) (Fig. 9) Kondo et al. (2003) (Fig. 7) Moran et al. (1987) (Fig. 5) Mesulan and Mufson (1982) (Fig. 1) Mufson and Mesulan (1982) (Fig. 1)	Saleem et al. (2008) (Fig. 9) Kondo et al. (2003) (Fig. 13) Mesulan and Mufson (1982) (Fig. 1) Mufson and Mesulan (1982) (Fig. 1)

(*continued*)

Table 4 Continued

Connecting area	TGdd[a]	TGdg	TGsts	TGvg	TGvd	TGa
	Mufson and Mesulan (1982) (Fig. 1)					
Middle insula	Moran et al. (1987) (Figs 4 and 8) Mufson and Mesulan (1982) (Fig. 3)	Moran et al. (1987) (Fig. 8) Mesulan and Mufson (1982) (Fig. 4) Mufson and Mesulan (1982) (Fig. 5)	Mesulan and Mufson (1982) (Fig. 5) Mufson and Mesulan (1982) (Fig. 3)	Mesulan and Mufson (1982) (Fig. 5) Mufson and Mesulan (1982) (Fig. 3)	Mufson and Mesulan (1982) (Fig. 3)	Mesulan and Mufson (1982) (Fig. 4) Mufson and Mesulan (1982) (Fig. 3)
Posterior insula	Mufson and Mesulan (1982) (Fig. 4)		Mesulan and Mufson (1982) (Fig. 3) Mufson and Mesulan (1982) (Fig. 4)		Mesulan and Mufson (1982) (Fig. 3) Moran et al. (1987) (Fig. 5) Mufson and Mesulan (1982) (Fig. 4)	Mesulan and Mufson (1982) (Fig. 3) Mufson and Mesulan (1982) (Fig. 4)
Temporal lobe						
Superior temporal gyrus	Saleem et al. (2008) (Fig. 6) Schmahmann and Pandya (2006) (Case 10) Muñoz and Insausti (2005) (Fig. 8) Kondo et al. (2003) (Figs 14 and 15) Moran et al. (1987) (Figs 4 and 8)	Saleem et al. (2008) (Fig. 6) Schmahmann and Pandya (2006) (Cases 10 and 11) Muñoz and Insausti (2005) (Fig. 8) Kondo et al. (2003) (Fig. 14) Seltzer and Pandya (1994) (Case 2) Moran et al. (1987) (Figs 3 and 8) Galaburda and Pandya (1983) (Figs 6 and 7)	Muñoz and Insausti (2005) (Fig. 8) Kondo et al. (2003) (Fig. 14) Galaburda and Pandya (1983) (Figs 6 and 7)	Muñoz and Insausti (2005) (Fig. 8)	Muñoz and Insausti (2005) (Fig. 8) Moran et al. (1987) (Fig. 5)	Saleem et al. (2008) (Fig. 6) Muñoz and Insausti (2005) (Fig. 8)
Superior temporal sulcus		Schmahmann and Pandya (2006) (Cases 10 and 11) Seltzer and Pandya (1994) (Cases 2–12 and 14) Seltzer and Pandya (1989) (Case 3) Moran et al. (1987) (Fig. 3) Galaburda and Pandya (1983) (Figs 6 and 7)	Kondo et al. (2003) (Fig. 14) Seltzer and Pandya (1994) (Cases 2–12, 14, 16, and 18) Seltzer and Pandya (1989) (Case 3) Galaburda and Pandya (1983) (Figs 6 and 7)	Saleem et al. (2008) (Fig. 6) Schmahmann and Pandya (2006) (Case 14) Kondo et al. (2003) (Fig. 15) Seltzer and Pandya (1994) (Cases 16 and 18) Seltzer and Pandya (1989) (Case 14)	Saleem et al. (2008) (Fig. 6) Kondo et al. (2003) (Fig. 14) Seltzer and Pandya (1994) (Cases 3, 4, and 6) Moran et al. (1987) (Fig. 5)	
Inferior temporal gyrus		Schmahmann and Pandya (2006) (Case 11) Webster et al. (1991) (Fig. 14) Moran et al. (1987) (Figs 3 and 9)	Schmahmann and Pandya (2006) (Case 15) Kondo et al. (2003) (Fig. 14) Webster et al. (1991) (Fig. 14) Moran et al. (1987) (Fig. 9)	Schmahmann and Pandya (2006) (Cases 15 and 16) Kondo et al. (2003) (Fig. 15) Webster et al. (1991) (Figs 9, 11, and 14) Moran et al. (1987) (Fig. 9)	Schmahmann and Pandya (2006) (Case 15) Kondo et al. (2003) (Fig. 14) Moran et al. (1987) (Figs 5 and 9)	Schmahmann and Pandya (2006) (Case 15) Moran et al. (1987) (Fig. 9)
Entorhinal cortex	Muñoz and Insausti (2005) (Figs 7 and 8) Kondo et al. (2003) (Fig. 14) Moran et al. (1987) (Figs 4 and 8)	Muñoz and Insausti (2005) (Fig. 8) Kondo et al. (2003) (Fig. 14) Moran et al. (1987) (Figs 3 and 8)	Kondo et al. (2003) (Fig. 14)	Insausti and Amaral (2008) (Fig. 15) Muñoz and Insausti (2005) (Fig. 8) Moran et al. (1987) (Fig. 8)	Insausti and Amaral (2008) (Fig. 15) Kondo et al. (2003) (Fig. 14) Moran et al. (1987) (Figs 5 and 8)	Moran et al. (1987) (Fig. 8)
Perirhinal cortex	Muñoz and Insausti (2005) (Figs 7 and 8) Lavenex et al. (2004) (Fig. 3) Kondo et al. (2003) (Figs 14 and 15) Moran et al. (1987) (Fig. 4)	Schmahmann and Pandya (2006) (Case 11) Muñoz and Insausti (2005) (Fig. 8) Kondo et al. (2003) (Fig. 14)	Kondo et al. (2003) (Fig. 14) Kondo et al. (2005) (Fig. 16)	Kondo et al. (2005) (Fig. 16) Muñoz and Insausti (2005) (Fig. 8) Lavenex et al. (2004) (Fig. 3) Kondo et al. (2003) (Fig. 15)	Kondo et al. (2005) (Fig. 16) Lavenex et al. (2004) (Fig. 3) Kondo et al. (2003) (Fig. 14) Moran et al. (1987) (Fig. 5)	Kondo et al. (2005) (Fig. 16) Lavenex et al. (2004) (Fig. 3)
Parahippocampal cortex	Muñoz and Insausti (2005) (Figs 7 and 8) Kondo et al. (2005) (Fig. 16) Kondo et al. (2003) (Figs 14 and 15) Moran et al. (1987) (Fig. 4)	Schmahmann and Pandya (2006) (Case 13) Muñoz and Insausti (2005) (Fig. 8) Kondo et al. (2005) (Fig. 16) Kondo et al. (2003) (Fig. 14) Moran et al. (1987) (Figs 3 and 9)		Lavenex et al. (2004) (Fig. 3) Moran et al. (1987) (Case 9)	Lavenex et al. (2004) (Fig. 3) Moran et al. (1987) (Fig. 5)	Kondo et al. (2005) (Fig. 16) Lavenex et al. (2004) (Fig. 3) Moran et al. (1987) (Fig. 9)
Hippocampus	Moran et al. (1987) (Fig. 4)	Insausti and Muñoz (2001) (Fig. 8) Moran et al. (1987) (Fig. 3)	Insausti and Muñoz (2001) (Fig. 8)	Insausti and Muñoz (2001) (Fig. 8)	Moran et al. (1987) (Fig. 5)	
Amygdala	Hoistad and Barbas (2008) (Fig. 2) Kondo et al. (2003) (Figs 14 and 15) Stefanacci et al. (1996) (Figs 17 and 18)	Hoistad and Barbas (2008) (Fig. 2) Schmahmann and Pandya (2006) (Case 11) Kondo et al. (2003) (Fig. 14)	Hoistad and Barbas (2008) (Fig. 2) Kondo et al. (2003) (Fig. 14) Amaral and Price (1984) (Figs 4 and 6)	Hoistad and Barbas (2008) (Fig. 2) Kondo et al. (2003) (Fig. 15) Stefanacci et al. (1996) (Fig. 17)	Hoistad and Barbas (2008) (Fig. 2) Kondo et al. (2003) (Fig. 14)	Hoistad and Barbas (2008) (Fig. 2) Stefanacci et al. (1996) (Figs 17 and 18) Amaral and Price (1984) (Figs 4 and 6)

(*continued*)

Table 4 Continued

Connecting area	TGdd[a]	TGdg	TGsts	TGvg	TGvd	TGa
	Moran et al. (1987) (Fig. 4) Amaral and Price (1984) (Figs 4 and 6) Herzog and Van Hoesen (1976) (Figs 1 and 6)	Moran et al. (1987) (Fig. 3) Amaral and Price (1984) (Figs 4 and 6) Herzog and Van Hoesen (1976) (Figs 2 and 6)	Herzog and Van Hoesen (1976) (Fig. 6)	Amaral and Price (1984) (Figs 4 and 6) Herzog and Van Hoesen (1976) (Fig. 6)	Stefanacci et al. (1996) (Figs 4, 11–14, 17, and 18) Moran et al. (1987) (Fig. 5) Amaral and Price (1984) (Figs 4 and 6) Herzog and Van Hoesen (1976) (Fig. 6)	Herzog and Van Hoesen (1976) (Fig. 6)
Basal ganglia						
Caudate	Kondo et al. (2003) (Fig. 10) Van Hoesen et al. (1981) (Cases 1 and 2)	Schmahmann and Pandya (2006) (Case 11) Yeterian and Pandya (1998) (Case 5) Van Hoesen et al. (1981) (Case 4)	Kondo et al. (2003) (Fig. 11)	Van Hoesen et al. (1981) (Case 6)		
Putamen	Kondo et al. (2003) (Fig. 10) Van Hoesen et al. (1981) (Cases 1 and 2)	Schmahmann and Pandya (2006) (Case 11) Yeterian and Pandya (1998) (Case 5) Van Hoesen et al. (1981) (Case 4)	Kondo et al. (2003) (Fig. 11)	Van Hoesen et al. (1981) (Case 6)		
Nucleus accumbens	Kondo et al. (2003) (Fig. 10) Van Hoesen et al. (1981) (Cases 1 and 2)	Van Hoesen et al. (1981) (Case 4)	Kondo et al. (2003) (Fig. 11)			
Claustrum	Moran et al. (1987) (Fig. 4)	Schmahmann and Pandya (2006) (Case 11) Moran et al. (1987) (Fig. 3)			Moran et al. (1987) (Fig. 5)	
Basal forebrain	Moran et al. (1987) (Fig. 4)	Schmahmann and Pandya (2006) (Case 11) Moran et al. (1987) (Fig. 3)			Moran et al. (1987) (Fig. 5)	
Thalamus						
Medial geniculate nucleus	Moran et al. (1987) (Fig. 4)	Schmahmann and Pandya (2006) (Case 11) Pandya et al. (1994) (Case 1) Moran et al. (1987) (Fig. 3)	Pandya et al. (1994) (Case 1)			
Lateral geniculate nucleus		Schmahmann and Pandya (2006) (Case 11) Pandya et al. (1994) (Case 1)	Pandya et al. (1994) (Case 1)			
Suprageniculate nucleus		Schmahmann and Pandya (2006) (Case 11) Pandya et al. (1994) (Case 1) Yeterian and Pandya (1991) (Case 1)	Pandya et al. (1994) (Case 1) Yeterian and Pandya (1991) (Case 1)			
Medial dorsal nucleus	Gower (1989) (Fig. 8)	Pandya et al. (1994) (Case 1) Yeterian and Pandya (1991) (Case 1) Moran et al. (1987) (Fig. 3)	Pandya et al. (1994) (Case 1) Yeterian and Pandya (1991) (Case 1)			Gower (1989) (Fig. 8)
Nucleus limitans	Moran et al. (1987) (Fig. 4)	Yeterian and Pandya (1991) (Case 1) Moran et al. (1987) (Fig. 3)	Yeterian and Pandya (1991) (Case 1 and 12)	Yeterian and Pandya (1991) (Case 12)	Moran et al. (1987) (Fig. 5)	
Medial pulvinar	Yeterian and Pandya (1989) (Case 1) Moran et al. (1987) (Fig. 4)	Schmahmann and Pandya, (2006) (Case 11) Pandya et al. (1994) (Case 1) Yeterian and Pandya (1991) (Case 1) Yeterian and Pandya (1989) (Case 1) Moran et al. (1987) (Fig. 3)	Pandya et al. (1994) (Case 1) Yeterian and Pandya (1991) (Case 1 and 12) Yeterian and Pandya (1989) (Cases 1 and 9)	Yeterian and Pandya (1991) (Case 12)	Moran et al. (1987) (Fig. 5)	
Hypothalamus	Moran et al. (1987) (Fig. 4)	Moran et al. (1987) (Fig. 3)			Moran et al. (1987) (Fig. 5)	
Brainstem		Schmahmann and Pandya (1991) (Case 1)	Schmahmann and Pandya (1991) (Case 1)			

[a]The macaque cytoarchitectonic nomenclature corresponds to that used by Kondo et al. (2003) and by Moran et al. (1987). TGdd and TGdg may correspond to TG and TAr in humans, respectively. TGa appears to correspond to area TI in humans. TGvd may correspond to anterior areas 35 and 36 of the human TP. TGvg and lower TGsts would correspond roughly to anterior area TE. Upper TGsts appears to correspond to the small anterior area TAp in humans. Within the table, in parenthesis after the citations, are the cases or figures relevant to TP connectivity.

TGvd (Corresponding to Anterior Areas 35 and 36)

Although in the macaque tract-tracing literature there are no tracer injections in the most rostral perirhinal cortex, there was a strong similarity between the perirhinal cortex RSFC in humans and the anatomical connectivity corresponding to tracer injections in TGvd of the macaque, located at diverse mediolateral and

rostrocaudal positions (Moran et al. 1987; Lavenex et al. 2002, 2004; Kondo et al. 2005): TGvd exhibited anatomical connectivity preferentially with the inferior temporal gyrus, as well as the rostral superior temporal gyrus, parahippocampal cortices, and with the orbitofrontal cortex. As in humans, Moran et al. (1987) (Case C) observed anatomical connectivity of the perirhinal cortex in the macaque monkey with areas that are intermediate between the orbital and medial prefrontal cortex. Perirhinal connections with the hippocampus, amygdala, and EC were also present in the macaque (Amaral and Price 1984; Stefanacci et al. 1996; Kondo et al. 2005; Hoistad and Barbas 2008). No studies about connectivity of the perirhinal region with the brainstem were found in the anatomical tracing literature.

EC and TGa (Corresponding to Anterior EC and Area TI)

The RSFC observations were consistent with those of anatomical tracing studies of areas EC and TGa in the macaque monkey, in that the anatomical connectivity also includes the hippocampus, amygdala, perirhinal, and parahippocampal cortices, medial frontal and orbitofrontal cortices, and the rostral part of the multimodal area of the STS (Munoz and Insausti 2005; Hoistad and Barbas 2008; Insausti and Amaral 2008). As in humans, in the macaque more moderate EC anatomical connectivity is directed to the caudal superior temporal gyrus, inferior temporal gyrus, parietal cortex, and little to the lateral frontal cortex, cingulate and anterior dysgranular insula (Munoz and Insausti 2005; Insausti and Amaral 2008). As with the perirhinal cortex, no studies about the connectivity between brainstem and EC or TGa were found in the anatomical tracing literature.

TGdd and TGvg Plus the Lower TGsts (Corrresponding to TG and Anterior Area TE)

The RSFC observations on TE and TG were remarkably consistent with the macaque tracing literature (Kondo et al. 2003; Saleem et al. 2008). As in humans, TGdd and TGvg in the macaque monkey are anatomically connected with well-defined cortical and subcortical circuits related to the medial prefrontal cortex and amygdala (Price and Drevets 2010). This network consists of areas on the ventromedial surface of the frontal cortex, areas along the medial edge of the orbital cortex, and a small caudolateral orbital region at the rostral end of the insula (Figs 4 and 10 in Kondo et al. (2003)). In addition, as in the case of anterior TE and TG in humans, the medial network is connected to a very specific set of other cortical regions, particularly the rostral part of the superior temporal gyrus and dorsal bank of the STS, the anterior and posterior cingulate gyrus (including some regions of the precuneus), the amygdala, the hippocampus, and the perirhinal and parahippocampal gyrus (Figs 4 and 5 in Saleem et al. (2008) and Webster et al. (1991)). As in human RSFC, macaque dorsolateral prefrontal cortex is interconnected with the medial prefrontal network (Case 4 in Petrides and Pandya (1999)). This network in the macaque is also characterized by its anatomical connectivity with other subcortical regions which demonstrated RSFC with the rostrolateral region of the TP in humans, such as the nucleus accumbens, the pulvinar, and the hypothalamus (Moran et al. 1987; Yeterian and Pandya 1991).

Discussion

Based on connectional studies in nonhuman primates and a recent tractography study in humans, the TP is hypothesized to be a convergence zone in which information from sensory, association, and limbic systems is integrated (Moran et al. 1987; Binney et al. 2012). Here, we support this hypothesis with data from functional connectivity MRI which demonstrates that the human TP is composed of multiple subregions with distinct connectional profiles, anchoring a set of 4 large-scale sensory, association, and paralimbic brain networks. The localization of the connectionally defined subregions of the TP was remarkably congruent with cytoarchitectural subdivisions r ecently described by (Ding et al. 2009). We will first discuss our results in more detail and consider their functional implications. Finally, we will comment on how the present data compare with anatomical connectivity studies.

Functional Implications of TP Connectivity

Although in this analysis the seeds were placed in the left TP, connectivity was most often bilateral and remarkably symmetrical, with the most notable exception of anterior area TA, represented by seed 6, which had stronger connectivity with the left fronto-parieto-temporal perisylvian association cortex, related to language. Connectivity of area TG with the default-semantic network was bilaterally symmetrical, but this area, at the tip of the TP and a hub to which all other seeds connected, had preferential ipsilateral connectivity to the dorsolateral prefrontal cortex and contralateral "cognitive" cerebellum. The mostly bilaterally symmetrical connectivity pattern of the TP is reflected in the cognitive and behavioral correlates of lesions in the TP. Despite some debate in the literature and a smattering of case report exceptions, where bilateral involvement by seizures cannot be discounted (Anson and Kuhlman 1993; Ghika-Schmid et al. 1995; Glosser et al. 2000), both, in monkeys and in humans, bilateral lesions are usually thought to be required for prominent clinical manifestations to be observed (Klüver and Bucy 1939; Lilly et al. 1983). An exception is language: in keeping with the more lateralized connectivity pattern we describe for area TA, heavily connected to perisylvian cortex, the semantic aspects of language are more likely to be affected by left-sided lesions (Damasio et al. 2004; Schwartz et al. 2009; Lambon Ralph et al. 2010). In addition, verbal semantic processing is impaired by predominantly left-sided TP disorders, while nonverbal semantic processing tends to be affected when the right TP is more involved (Butler et al. 2009). Likewise, semantic tasks involving auditory stimuli tend to more robustly activate the left TP (Visser and Lambon Ralph 2011). However, in most lesion cases, there is either damage of regions of the left hemisphere outside the TP or bilateral TP damage; purely unilateral left-sided TP lesions are unlikely to cause clinical semantic impairment, even during the acute stage (Tsapkini et al. 2011).

Anterior Area TA, on the Dorsal Aspect of the TP

Anterior area TA is represented by 2 seeds, one more posteriorly, seed 40, which given the inclination of the coronal sections on MRI (Fig. 1) could actually be located in area TA, and one more anteriorly, seed 6. The connectivity of anterior area TA suggests an important role in the integration of auditory information (Griffiths et al. 1998; Glosser et al. 2000) with somatosensory function corresponding to the mouth and hand. Although

some of this somatosensory–auditory integration—critical for the formation of "auditory objects"—seems to occur independently of TP function (Griffiths and Warren 2004; Rauschecker and Scott 2009), the TP may modulate sensorimotor–auditory integration or may further process this integrated information to categorize "auditory objects" or a combination of objects to form concepts (Pobric et al. 2010; Baron and Osherson 2011). The most posterior portion (seed 40) of anterior TA was linked to primary cortex, whereas its most anterior portion (seed 6) connected to association cortex surrounding the primary cortex linked to seed 40. This postero-anterior gradient represents yet another example in the brain of the hierarchical arrangement described for the frontal lobe, where more caudal structures support more concrete tasks, while more rostral regions support higher order processes underlying more abstract tasks (Badre et al. 2009). The higher order regions tend to receive greater input from "motivational" or limbic regions, as is the case with the anterior portion of TA, and still more with TG, to which TA is richly connected. Our data demonstrating connectivity of TA with multiple other areas of the large-scale language network are consistent with functional neuroimaging studies showing activation of the dorsal aspect of the left TP during tasks such as the identification of proper famous names (Gorno-Tempini et al. 1998) and other paradigms of auditory semantic processing (Binder et al. 1999) (Visser and Lambon Ralph 2011). Furthermore, although semantic dementia exerts its earliest effects in the basal portion of the TP (Butler et al. 2009), dorsal TP damage correlates best with semantic and lexical impairment (Wilson et al. 2010). Clinical findings with TP pathology are striking, for instance: "patients with damage to the anterior sector of the left temporal lobe, involving the TP, in spite of [having] fluent and non-aphasic language, were impaired in the retrieval of names for specific persons. The patients knew who the person was and provided verbal descriptions that allowed an independent examiner, who did not know what stimulus the patient was looking at, to guess which person the patient was trying to name" (Damasio et al. 2004). This description indicates that visual processing per se was not affected by the TP lesion. Our data indicate that visual pathways are not functionally related to region TA, which however could be the key node of a network linking auditory cortex, critical for the processing of semantic verbal information, with the perisylvian regions of the left frontal and parietal lobes, critical for speech production. Patients with lesions in the left TP, or with dysfunction produced here by transcranial magnetic stimulation, tend to be most impaired in recognizing and, particularly, naming unique entities, for instance, a specific person or the make of a car, but they are also impaired at more general levels of naming categories (Damasio et al. 2004; Patterson et al. 2007). In cognitive neuroscience, the TP has been proposed as the hub linking multiple streams of modality-specific sensory information into multimodal conceptual representations (Patterson et al. 2007; Baron and Osherson 2011; Lambon Ralph et al. 2011). It is possible that area TA, in the dorsal aspect of the TP, plays a major role in semantic auditory information processing, while areas TE and TG, in the basolateral aspect and tip of the TP, are more critical in binding multimodal information and thus providing modality-invariant representations (Baron and Osherson 2011; Visser and Lambon Ralph 2011; Visser et al. 2012). The importance of anterior area TA for language may explain its greater development in the human brain when compared with nonhuman primates. Among other features, in the human dorsomedial aspect of the TP, there is a steep change in thickness between the thicker cortex of this area and the neighboring cortex, giving rise to the shallow semicircular notch we describe (Supplementary Figs 1 and 2). This notch does not seem to be present even in highly evolved nonhuman primates, such as the baboon (Blaizot et al. 2004).

Other than EC, anterior TA was the only TP region connected to the insula. The pattern of functional connectivity parallels structural connectivity findings, with its most posterior portion connecting to the entire insula and its most anterior portion only to the anterior insula (Cloutman et al. 2012).

Anterior Areas 35 and 36

The connectivity of seeds 34 and 25, in anterior perirhinal cortex, confirms findings in nonhuman primates suggesting that this area plays an important role in visual processing, including complex pattern recognition and form analysis necessary for object identification (Murray and Richmond 2001). The connectivity of area 35, linked not only to anterior hippocampus, as other TP regions, but also to posterior hippocampus and parahippocampal cortex, is compatible with the view that this portion of the TP may be a higher order representational component of the ventral visual cortical-perirhinal-hippocampal stream (Cowell et al. 2010). However, it is remarkable that for areas deemed to be critical in visual processing, no RSFC with the classical visual areas, such as BA 18 and 19, was detected in either area 35 or 36. This finding suggests that intermediate regions, such as BA 37, forward visual information rostrally to BA 20, which has RSFC with both anterior areas 35 and 36. This possibility is supported by tractography studies in semantic dementia, with prominent damage of the basal TP and yet sparing of the inferior longitudinal fasciculus caudal to the anterior temporal region (Acosta-Cabronero et al. 2011). The strong connectivity of area 36 with subcortical structures involved in salience mechanisms, such as ventral tegmental area, nucleus accumbens, amygdala, and medial globus pallidus, suggests that it may play a role in the assessment of the value or relevance of visual and other information. This is particularly likely in the case of area 35, with RSFC to the periaqueductal gray, of critical importance for eye-movement control. Suggesting further a role in eye-movement control was the exclusive connectivity among TP areas of areas 35 and 36 to the vestibular nuclei; areas 35 and 36 were also connected to the anterior hippocampus, known to mediate vestibular processing in humans (Hufner et al. 2011). One possible hypothesis would be that these TP areas modulate the vestibular system to reduce or enhance the level of vestibular control over eye movements, depending on prior knowledge about requirements for interaction with specific objects identified visually. Finally, areas 35 and 36 are also strongly connected with areas TE and TG, both firmly integrated in the semantic network. Thus, these areas could provide a gateway for the semantic network to access higher order visual information and integrate it with information from other modalities, as suggested by convergent evidence from neuropsychological, fMRI and depth electrode studies that these anterior ventral areas are not exclusive to visual processing but seem to be implicated in core multimodal semantic representation (see, e.g., Thesen et al. 2012; Visser et al. 2012; Binney et al. 2010, 2012; Peelen and Caramazza 2012). While debate continues on this topic (Murray et al. 2007), areas 35 and 36 appear to be involved in higher order visual processing, semantic memory, and episodic memory especially for items (Allison

et al. 1999), as in the identification of visually presented unique (famous) faces or buildings (Grabowski et al. 2001).

Anterior EC and TI

Corresponding to their connectivity to olfactory cortex, EC and TI are the only cortical areas in the TP with thick myelinated olfactory fibers in layer Ia, somewhat more abundant in TI (Ding et al. 2009). Anterior EC shares with TI extensive bilateral connections to anterior temporal structures and orbitofrontal cortex, but the connectivity of EC suggests that it is more tightly linked to mnemonic and autonomic processes, whereas TI participates in a network involved in motivational processes. EC shows more robust connectivity than TI to the hippocampus and perirhinal cortex, consistent with its role in memory, while TI shows more robust connectivity than EC to olfactory and piriform cortex.

EC is connected to the entire hypothalamus and, probably through it, to the arcuate nucleus of the medulla, thought to be a chemodetector of hypoxia–hypercapnia in the CSF; neuronal loss here has been associated with sudden death (Zec et al. 1997; Benarroch 2003; Machaalani and Waters 2008; Tada et al. 2009). By contrast, TI connectivity to the bed nucleus of the stria terminalis, VTA, medial raphe nucleus and the region of the nucleus coeruleus, suggests that TI participates in motivational processes. The bed nucleus of the stria terminalis, functionally akin to the amygdala, is needed for the production of chronic anxiety in animal models (Davis et al. 2010). Well known are the roles of the dopaminergic VTA, serotoninergic medial raphe, and noradrenergic nucleus locus coeruleus in the mediation of reward and in influencing mood and generating anxiety (Cools et al. 2011). The shared connectivity may provide the opportunity for interaction between these 2 networks.

Anterior Area TE

Areas TE and TG shared connectivity within a large and distinct network (Fig. 3) that has been found to be related to semantic tasks (Binder et al. 2009) and some areas of which, not surprisingly, are also activated by social interactions (Simmons et al. 2010; Gotts et al. 2012; Regenbogen et al. 2012). Both TE and TG had RSFC with the amygdala, not emphasized as a component of the semantic network (Binder et al. 2009) but a prominent component of one of the key networks involved in social behavior (Adolphs 2009; Gotts et al. 2012). Many of the regions included in these networks are also part of the default mode network (Buckner et al. 2008). Among the temporal tip areas, TE was the only one connected to all other areas considered by Binder et al. (2009) to be part of the distributed network for semantic processing. Located at the rostral extent of the ventral visual and auditory pathways, TP cortex in a region consistent with area TE is activated by multimodal semantic tasks; thus, this region has been postulated to underpin the modality-invariant hub within the hub-and-spoke semantic framework (Visser and Lambon Ralph 2011; Visser et al. 2012). It is also critical for the categorization of semantically closely related items (e.g., "apple" vs. "pear") (Baron and Osherson 2011; Schwartz et al. 2011; Peelen and Caramazza 2012). In addition, area TE provides a bridge between the semantic network and some of the subcortical structures involved in emotional processes, including lateral amygdala and anterior hypothalamus. It has been activated by tasks that bridge the cognitive and emotional domains, such as the identification of various degrees of sadness in faces (Blair et al. 1999). The connectivity of area TE to the thalamic pulvinar suggests its role in the integration of visual information. Earlier neuroanatomical studies already showed in human strong connections between this region of the TP and the pulvinar through the temporopulvinar bundle of Arnold (Klingler and Gloor 1960), which can be demonstrated by gross dissection of the temporal white matter and which is also present in the macaque (Yeterian and Pandya 1991). The areas of the pons and cerebellum connected to area TE correspond to the neocerebellum, known to participate in cognitive functions (Stoodley and Schmahmann 2010). The most caudal portion of Crus I and II, connected to TE and TG with a contralateral predominance, as expected for cerebello-hemispheric connectivity, has been specifically activated by semantic tasks (Devlin et al. 2000), including interpersonal speech content (Regenbogen et al. 2012), and found to be functionally connected to TP clusters activated by person-selective tasks (Simmons et al. 2010).

Area TG

The convergent role of area TG, at the anterior tip of the TP, is suggested by its rich connectivity to all the subregions of the TP. In fact, it was the only TP region with connectivity to all others. As in the frontal lobe (Badre et al. 2009), the convergence hub of the temporal lobe is placed in its most anterior tip. While both TE and TG demonstrated connectivity with part of the amygdala, the spatial patterns were disparate, with TE preferentially connected to lateral amygdala and TG to medial amygdala. Along with lateral orbitofrontal cortex, the lateral amygdala is critical for integrative sensory processing and these structures are probably involved with assigning value or relevance to highly processed visual information in TE; the medial amygdala shares connectivity with reward-related structures including the nucleus accumbens (to which TG also connects), suggesting a key role for TG in the integration of multimodal information with reward and approach-related behavior (Bickart et al. 2012). The importance of area TG for the coordination of personal and emotional information is suggested by studies showing activation of this area with theory of mind tasks (Baron-Cohen et al. 1999). Most subregions of the TP had RSFC to TG, in the very anterior tip of the TP, a likely coordinating hub, with strong RSFC to the semantic network. TG was the only subregion of the TP—for that matter, the only region of the entire brain—which demonstrated RSFC to most of the other subregions we mapped in the TP.

Comparison of Anatomical Connectivity in Monkey and Humans with Functional Connectivity in Humans

The TP is a brain structure exclusively present in human and nonhuman primates. Among primates, the increasing development of the TPs correlates with the development of the cortical mantle, increasing in size and complexity in more evolved nonhuman primate species (Markowitsch et al. 1985; Blaizot et al. 2004) to reach maximal size and complexity in humans (Ding et al. 2009; Blaizot et al. 2010). Given the anatomical and functional differences between species, caution is necessary when considering possible homologous connectional patterns (Gloor 1997).

Although many studies have traced the anatomical connectivity of the TP in monkey (see the Results section and Supplementary Table 2), only 2 have addressed the anatomical connectivity of specific cytoarchitectonic regions (Moran et al.

1987; Kondo et al. 2003). Both studies demonstrated that the dorsolateral part of the TP, particularly involved in auditory processing, is mainly interconnected with the auditory areas of the superior temporal cortex and with the medial prefrontal cortex, while the ventromedial part, preferentially involved in visual processing, is interconnected with the visual areas of the inferior temporal cortex and with the orbitofrontal cortex. These general principles are largely maintained in the human TP, but there are some differences as well. As in primates, the dorsal TP in humans showed RSFC mainly with the auditory areas of the superior temporal cortex and also with the medial prefrontal cortex, but in this case not with the ventromedial but rather the dorsomedial surface of prefrontal cortex. Areas TG and anterior TE did show strong RSFC with the ventromedial prefrontal cortex, as well as with the rest of the areas included in the semantic network. These 2 areas, TG and anterior area TE, are difficult to identify in the macaque monkey. TG, in particular, is very poorly represented in the macaque (Von Bonin and Bailey 1947), and is sometimes identified as area TGdd, located in the dorsomedial TP (Kondo et al. 2003). Anterior area TE is more ventral and smaller in monkeys than in humans because in the macaque there are only 2 gyri, superior and inferior, in the lateral aspect of the temporal lobe, rather than the 3 gyri present in humans. Similar to the macaque monkey, the ventromedial TP in humans showed RSFC mainly with visual and paralimbic areas. As in the monkey, the entire TP showed strong RSFC with the amygdala and the entorhinal and perirhinal cortices. A fuller comparative analysis of TP connectivity across the 2 species is beyond the scope of this article.

Our findings strongly agree with a recent study using diffusion tensor tractography to investigate the connectivity of the human TP (Binney et al. 2012). The pattern of intratemporal connectivity in this study suggested that multimodal sensory information encoded in the caudal temporal cortex gradually converges moving rostrally to reach the temporal polar cortex, where information becomes maximally mixed (Binney et al. 2012). In our study, the polar area, TG, is characterized by being connected to all the other areas of the TP. Areas TG and TA, in the rostral superior temporal gyrus, had extensive connectivity with frontoparietal areas, which were not connected to seeds located in the inferior portion of the TP. Similarly, in their midtemporal section (near our most caudal seed locations), Binney et al. (2012) detected pathways to the frontoparietal regions only from the superior temporal gyrus. Finally, they report a tract connecting the temporopolar areas to the orbital portion of the inferior frontal gyrus (Binney et al. 2012); this tract (considered part of the uncinate fasciculus) likely underlies the functional connectivity we observed between areas TG and TA and a similar region of the frontal lobe. Even though the findings in this diffusion tensor tractography study are very similar to those of the present functional connectivity investigation, it is worth noting that the 2 techniques may provide distinct and potentially complementary information since functional connectivity findings may traverse multiple synapses or may show correspondence between 2 regions not directly connected but rather connected to a common third region.

Limitations

This study has several limitations. Unlike tract-tracing studies in monkeys, functional connectivity, similarly to diffusion tensor imaging, does not allow for the determination of the direction in which 2 regions are connected. However, unless performed with tracers such as the rabies virus, animal tracing studies are limited to one synaptic link, while functional connectivity depicts an array of regions potentially connected by a series of synaptic links. Thus, functional connectivity provides a fuller picture of the network relationships of any given region. Another potential limitation is that we do not display connectivity patterns at a range of correlation strengths, as done in studies involving regions such as the striatum (Choi et al. 2012), with much better known connectivity than the TP. Given the novelty and anatomical complexity of the networks depicted at the z value we chose, commonly employed in functional connectivity studies (Van Dijk et al. 2010; Buckner et al. 2011), we elected to display the data at a single threshold value. However, as in other functional connectivity studies (Yeo et al. 2011), we obtained similar network findings (not shown) at a range of z values around the chosen threshold. Another important limitation relates to the fact that we did not employ an advanced nonlinear registration algorithm, such as DARTEL or ANTS, to register each individual subject's data to the MNI template. It is possible that this resulted in the blurring of some boundaries in the TP, a notoriously anatomically heterogeneous cortical region across individuals. This would have reduced the specificity of our large-scale network findings and presumably would have biased against finding correspondence between the clustering of TP seeds in the present data and the cytoarchitectural findings reported previously by Ding et al. (2009). In the same direction would lead another potential limitation of our method: although the SNR reached a level adequate for fMRI (Murphy et al. 2007), newer techniques that optimize SNR for the TP may be applied in future studies (Binney et al. 2012). Finally, the detail of the connectivity patterns we describe is limited by the voxel resolution of the optimized EPI sequences we used in a 3T scanner. It is possible that a more detailed and accurate rendition of the connectivity of the TP may be obtained with a higher field strength scanner, once the difficulties posed by susceptibility artifacts in the TP region are properly addressed.

Conclusions

In summary, the parcellation of the human TP using large-scale functional connectivity yielded a complex set of subregions, strikingly coincident with the cytoarchitectonic subregions recently mapped in postmortem human tissue. Despite the complexity, the patterns that emerged from these data indicated the presence of 4 large-scale brain networks anchored within the human TP: 1) a dorsal network, with predominant connectivity to auditory and somato-sensorimotor regions, particularly those involved with language; 2) a ventromedial network, predominantly connected to higher level visual regions; 3) a medial network, connected to paralimbic structures; and 4) an anterolateral network, connected to the default-semantic network. Although 4 distinct networks were detected, the transitions between large-scale connectional patterns with TP seeds were gradual, in keeping with the gradual changes in cytoarchitecture in the TP. All subregions of the TP were connected to the small area at the very rostral tip of the TP, likely an important convergence hub. Most of the connectivity maps were quite symmetrical, except for the map anchored in the dorsal, language-related, subregion. The highly specific connectivity of different subregions

with subcortical structures, such as the hypothalamus or the ventral tegmental area of the midbrain, are only some of the newly discovered relationships provided by this study which should be further explored in future work.

Supplementary Material

Supplementary material can be found at: http://www.cercor.oxfordjournals.org/.

Funding

Supported by grants from the National Institute on Aging (P50-AG005134) and National Institute of Neurological Disorders and Stroke (R21-NS077059).

Notes

Conflict of Interest: None declared.

References

Acosta-Cabronero J, Patterson K, Fryer TD, Hodges JR, Pengas G, Williams GB, Nestor PJ. 2011. Atrophy, hypometabolism and white matter abnormalities in semantic dementia tell a coherent story. Brain. 134:2025–2035.

Adolphs R. 2009. The social brain: neural basis of social knowledge. Annu Rev Psychol. 60:693–716.

Allison T, Puce A, Spencer DD, McCarthy G. 1999. Electrophysiological studies of human face perception. I: Potentials generated in occipitotemporal cortex by face and non-face stimuli. Cereb Cortex. 9:415–430.

Amaral DG, Price JL. 1984. Amygdalo-cortical projections in the monkey (Macaca fascicularis). J Comp Neurol. 230:465–496.

Anson JA, Kuhlman DT. 1993. Post-ictal Kluver-Bucy syndrome after temporal lobectomy. J Neurol Neurosurg Psychiatry. 56:311–313.

Badre D, Hoffman J, Cooney JW, D'Esposito M. 2009. Hierarchical cognitive control deficits following damage to the human frontal lobe. Nat Neurosci. 12:515–522.

Barbas H. 1988. Anatomic organization of basoventral and mediodorsal visual recipient prefrontal regions in the rhesus monkey. J Comp Neurol. 276:313–342.

Barbas H. 1993. Organization of cortical afferent input to orbitofrontal areas in the rhesus monkey. Neuroscience. 56:841–864.

Barbas H, Ghashghaei H, Dombrowski SM, Rempel-Clower NL. 1999. Medial prefrontal cortices are unified by common connections with superior temporal cortices and distinguished by input from memory-related areas in the rhesus monkey. J Comp Neurol. 410:343–367.

Baron SG, Osherson D. 2011. Evidence for conceptual combination in the left anterior temporal lobe. Neuroimage. 55:1847–1852.

Baron-Cohen S, Ring HA, Wheelwright S, Bullmore ET, Brammer MJ, Simmons A, Williams SC. 1999. Social intelligence in the normal and autistic brain: an fMRI study. Eur J Neurosci. 11:1891–1898.

Benarroch EE. 2003. Brainstem in multiple system atrophy: clinicopathological correlations. Cell Mol Neurobiol. 23:519–526.

Bickart KC, Hollenbeck MC, Barrett LF, Dickerson BC. 2012. Intrinsic amygdala-cortical functional connectivity predicts social network size in humans. J Neurosci. 32:14729–14741.

Bigler ED. 2007. Anterior and middle cranial fossa in traumatic brain injury: relevant neuroanatomy and neuropathology in the study of neuropsychological outcome. Neuropsychology. 21:515–531.

Binder JR, Desai RH, Graves WW, Conant LL. 2009. Where is the semantic system? A critical review and meta-analysis of 120 functional neuroimaging studies. Cereb Cortex. 19:2767–2796.

Binder JR, Frost JA, Hammeke TA, Bellgowan PS, Rao SM, Cox RW. 1999. Conceptual processing during the conscious resting state. A functional MRI study. J Cogn Neurosci. 11:80–95.

Binney RJ, Embleton KV, Jefferies E, Parker GJ, Ralph MA. 2010. The ventral and inferolateral aspects of the anterior temporal lobe are crucial in semantic memory: evidence from a novel direct comparison of distortion-corrected fMRI, rTMS, and semantic dementia. Cereb Cortex. 20:2728–2738.

Binney RJ, Parker GJ, Lambon Ralph MA. 2012. Convergent connectivity and graded specialization in the rostral human temporal lobe as revealed by diffusion-weighted imaging probabilistic tractography. J Cogn Neurosci. 24:1998–2014.

Biswal B, Yetkin FZ, Haughton VM, Hyde JS. 1995. Functional connectivity in the motor cortex of resting human brain using echo-planar MRI. Magn Reson Med. 34:537–541.

Blair RJ, Morris JS, Frith CD, Perrett DI, Dolan RJ. 1999. Dissociable neural responses to facial expressions of sadness and anger. Brain. 122(Pt 5):883–893.

Blaizot X, Mansilla F, Insausti AM, Constans JM, Salinas-Alaman A, Pro-Sistiaga P, Mohedano-Moriano A, Insausti R. 2010. The human parahippocampal region: I. temporal pole cytoarchitectonic and MRI correlation. Cereb Cortex. 20:2198–2212.

Blaizot X, Martinez-Marcos A, Arroyo-Jimenez Md Mdel M, Marcos P, Artacho-Perula E, Munoz M, Chavoix C, Insausti R. 2004. The parahippocampal gyrus in the baboon: anatomical, cytoarchitectonic and magnetic resonance imaging (MRI) studies. Cereb Cortex. 14:231–246.

Brodmann K. 1909. Vergleichende Lokalisationslehere der Grosshimrinde in ihren Principien dargestellt auf des Grund des Zellenbayes. Leipzig: Barth.

Buckner RL, Andrews-Hanna JR, Schacter DL. 2008. The brain's default network: anatomy, function, and relevance to disease. Ann N Y Acad Sci. 1124:1–38.

Buckner RL, Krienen FM, Castellanos A, Diaz JC, Yeo BT. 2011. The organization of the human cerebellum estimated by intrinsic functional connectivity. J Neurophysiol. 106:2322–2345.

Butler CR, Brambati SM, Miller BL, Gorno-Tempini ML. 2009. The neural correlates of verbal and nonverbal semantic processing deficits in neurodegenerative disease. Cogn Behav Neurol. 22:73–80.

Chabardes S, Kahane P, Minotti L, Tassi L, Grand S, Hoffmann D, Benabid AL. 2005. The temporopolar cortex plays a pivotal role in temporal lobe seizures. Brain. 128:1818–1831.

Choi EY, Yeo BT, Buckner RL. 2012. The organization of the human striatum estimated by intrinsic functional connectivity. J Neurophysiol. 108:2242–2263.

Cloutman LL, Binney RJ, Drakesmith M, Parker GJ, Lambon Ralph MA. 2012. The variation of function across the human insula mirrors its patterns of structural connectivity: evidence from in vivo probabilistic tractography. Neuroimage. 59:3514–3521.

Cohen AL, Fair DA, Dosenbach NU, Miezin FM, Dierker D, Van Essen DC, Schlaggar BL, Petersen SE. 2008. Defining functional areas in individual human brains using resting functional connectivity MRI. Neuroimage. 41:45–57.

Cools R, Nakamura K, Daw ND. 2011. Serotonin and dopamine: unifying affective, activational, and decision functions. Neuropsychopharmacology. 36:98–113.

Cowell RA, Bussey TJ, Saksida LM. 2010. Components of recognition memory: dissociable cognitive processes or just differences in representational complexity? Hippocampus. 20:1245–1262.

Damasio AR, Grabowski TJ, Bechara A, Damasio H, Ponto LL, Parvizi J, Hichwa RD. 2000. Subcortical and cortical brain activity during the feeling of self-generated emotions. Nat Neurosci. 3:1049–1056.

Damasio AR, Tranel D, Damasio H. 1990. Face agnosia and the neural substrates of memory. Annu Rev Neurosci. 13:89–109.

Damasio H, Grabowski TJ, Tranel D, Hichwa RD, Damasio AR. 1996. A neural basis for lexical retrieval. Nature. 380:499–505.

Damasio H, Tranel D, Grabowski T, Adolphs R, Damasio A. 2004. Neural systems behind word and concept retrieval. Cognition. 92:179–229.

Davis M, Walker DL, Miles L, Grillon C. 2010. Phasic vs sustained fear in rats and humans: role of the extended amygdala in fear vs anxiety. Neuropsychopharmacology. 35:105–135.

Devlin JT, Russell RP, Davis MH, Price CJ, Wilson J, Moss HE, Matthews PM, Tyler LK. 2000. Susceptibility-induced loss of signal: comparing PET and fMRI on a semantic task. Neuroimage. 11:589–600.

Dice LR. 1945. Measures of the amount of ecologic association between species. Ecology. 26:297–302.
Dickerson BC, Bakkour A, Salat DH, Feczko E, Pacheco J, Greve DN, Grodstein F, Wright CI, Blacker D, Rosas HD et al. 2009. The cortical signature of Alzheimer's disease: regionally specific cortical thinning relates to symptom severity in very mild to mild AD dementia and is detectable in asymptomatic amyloid-positive individuals. Cereb Cortex. 19:497–510.
Dickerson BC, Stoub TR, Shah RC, Sperling RA, Killiany RJ, Albert MS, Hyman BT, Blacker D, Detoledo-Morrell L. 2011. Alzheimer-signature MRI biomarker predicts AD dementia in cognitively normal adults. Neurology. 76:1395–1402.
Ding SL, Van Hoesen GW, Cassell MD, Poremba A. 2009. Parcellation of human temporal polar cortex: a combined analysis of multiple cytoarchitectonic, chemoarchitectonic, and pathological markers. J Comp Neurol. 514:595–623.
Evans JJ, Heggs AJ, Antoun N, Hodges JR. 1995. Progressive prosopagnosia associated with selective right temporal lobe atrophy. A new syndrome? Brain. 118(Pt 1):1–13.
Fletcher PC, Happe F, Frith U, Baker SC, Dolan RJ, Frackowiak RS, Frith CD. 1995. Other minds in the brain: a functional imaging study of "theory of mind" in story comprehension. Cognition. 57:109–128.
Fukatsu R, Fujii T, Tsukiura T, Yamadori A, Otsuki T. 1999. Proper name anomia after left temporal lobectomy: a patient study. Neurology. 52:1096–1099.
Galaburda AM, Pandya DN. 1983. The intrinsic architectonic and connectional organization of the superior temporal region of the rhesus monkey. J Comp Neurol. 221:169–184.
Ghika-Schmid F, Assal G, De Tribolet N, Regli F. 1995. Kluver-Bucy syndrome after left anterior temporal resection. Neuropsychologia. 33:101–113.
Gloor P. 1997. The temporal lobe and the limbic system. Oxford: Oxford University Press.
Glosser G, Salvucci AE, Chiaravalloti ND. 2003. Naming and recognizing famous faces in temporal lobe epilepsy. Neurology. 61: 81–86.
Glosser G, Zwil AS, Glosser DS, O'Connor MJ, Sperling MR. 2000. Psychiatric aspects of temporal lobe epilepsy before and after anterior temporal lobectomy. J Neurol Neurosurg Psychiatry. 68:53–58.
Gorno-Tempini ML, Price CJ, Josephs O, Vandenberghe R, Cappa SF, Kapur N, Frackowiak RS. 1998. The neural systems sustaining face and proper-name processing. Brain. 121(Pt 11):2103–2118.
Gorno-Tempini ML, Rankin KP, Woolley JD, Rosen HJ, Phengrasamy L, Miller BL. 2004. Cognitive and behavioral profile in a case of right anterior temporal lobe neurodegeneration. Cortex. 40:631–644.
Gotts SJ, Simmons WK, Milbury LA, Wallace GL, Cox RW, Martin A. 2012. Fractionation of social brain circuits in autism spectrum disorders. Brain. 135:2711–2725.
Gower EC. 1989. Efferent projections from limbic cortex of the temporal pole to the magnocellular medial dorsal nucleus in the rhesus monkey. J Comp Neurol. 280:343–358.
Grabowski TJ, Damasio H, Tranel D, Ponto LL, Hichwa RD, Damasio AR. 2001. A role for left temporal pole in the retrieval of words for unique entities. Hum Brain Mapp. 13:199–212.
Griffiths TD, Buchel C, Frackowiak RS, Patterson RD. 1998. Analysis of temporal structure in sound by the human brain. Nat Neurosci. 1:422–427.
Griffiths TD, Warren JD. 2004. What is an auditory object? Nat Rev Neurosci. 5:887–892.
Herzog AG, Van Hoesen GW. 1976. Temporal neocortical afferent connections to the amygdala in the rhesus monkey. Brain Res. 115:57–69.
Hickok G, Poeppel D. 2007. The cortical organization of speech processing. Nat Rev Neurosci. 8:393–402.
Hoistad M, Barbas H. 2008. Sequence of information processing for emotions through pathways linking temporal and insular cortices with the amygdala. Neuroimage. 40:1016–1033.
Horel JA, Keating EG, Misantone LJ. 1975. Partial Kluver-Bucy syndrome produced by destroying temporal neocortex or amygdala. Brain Res. 94:347–359.
Hufner K, Strupp M, Smith P, Brandt T, Jahn K. 2011. Spatial separation of visual and vestibular processing in the human hippocampal formation. Ann N Y Acad Sci. 1233:177–186.
Imaizumi S, Mori K, Kiritani S, Kawashima R, Sugiura M, Fukuda H, Itoh K, Kato T, Nakamura A, Hatano K et al. 1997. Vocal identification of speaker and emotion activates different brain regions. Neuroreport. 8:2809–2812.
Insausti R, Amaral DG. 2008. Entorhinal cortex of the monkey: IV. topographical and laminar organization of cortical afferents. J Comp Neurol. 509:608–641.
Insausti R, Juottonen K, Soininen H, Insausti AM, Partanen K, Vainio P, Laakso MP, Pitkanen A. 1998. MR volumetric analysis of the human entorhinal, perirhinal, and temporopolar cortices. AJNR Am J Neuroradiol. 19:659–671.
Insausti R, Munoz M. 2001. Cortical projections of the non-entorhinal hippocampal formation in the cynomolgus monkey (Macaca fascicularis). Eur J Neurosci. 14:435–451.
Kapur N, Barker S, Burrows EH, Ellison D, Brice J, Illis LS, Scholey K, Colbourn C, Wilson B, Loates M. 1994. Herpes simplex encephalitis: long term magnetic resonance imaging and neuropsychological profile. J Neurol Neurosurg Psychiatry. 57:1334–1342.
Kelly C, Uddin LQ, Shehzad Z, Margulies DS, Castellanos FX, Milham MP, Petrides M. 2010. Broca's region: linking human brain functional connectivity data and non-human primate tracing anatomy studies. Eur J Neurosci. 32:383–398.
Kimbrell TA, George MS, Parekh PI, Ketter TA, Podell DM, Danielson AL, Repella JD, Benson BE, Willis MW, Herscovitch P et al. 1999. Regional brain activity during transient self-induced anxiety and anger in healthy adults. Biol Psychiatry. 46:454–465.
Klingler J, Gloor P. 1960. The connections of the amygdala and of the anterior temporal cortex in the human brain. J Comp Neurol. 115:333–369.
Klüver H, Bucy P. 1939. Preliminary analysis of functions of the temporal lobes in monkeys. Arch Neurol Psychiat. 42:979–1000.
Kondo H, Saleem KS, Price JL. 2005. Differential connections of the perirhinal and parahippocampal cortex with the orbital and medial prefrontal networks in macaque monkeys. J Comp Neurol. 493:479–509.
Kondo H, Saleem KS, Price JL. 2003. Differential connections of the temporal pole with the orbital and medial prefrontal networks in macaque monkeys. J Comp Neurol. 465:499–523.
Lambon Ralph MA, Cipolotti L, Manes F, Patterson K. 2010. Taking both sides: do unilateral anterior temporal lobe lesions disrupt semantic memory? Brain. 133:3243–3255.
Lambon Ralph MA, Sage K, Jones RW, Mayberry EJ. 2011. Coherent concepts are computed in the anterior temporal lobes. Proc Natl Acad Sci USA. 107:2717–2722.
Landis JR, Koch GG. 1977. The measurement of observer agreement for categorical data. Biometrics. 33:159–174.
Lavenex P, Suzuki WA, Amaral DG. 2004. Perirhinal and parahippocampal cortices of the macaque monkey: intrinsic projections and interconnections. J Comp Neurol. 472:371–394.
Lavenex P, Suzuki WA, Amaral DG. 2002. Perirhinal and parahippocampal cortices of the macaque monkey: projections to the neocortex. J Comp Neurol. 447:394–420.
Lilly R, Cummings JL, Benson DF, Frankel M. 1983. The human Kluver-Bucy syndrome. Neurology. 33:1141–1145.
Machaalani R, Waters KA. 2008. Neuronal cell death in the Sudden Infant Death Syndrome brainstem and associations with risk factors. Brain. 131:218–228.
Margulies DS, Vincent JL, Kelly C, Lohmann G, Uddin LQ, Biswal BB, Villringer A, Castellanos FX, Milham MP, Petrides M. 2009. Precuneus shares intrinsic functional architecture in humans and monkeys. Proc Natl Acad Sci USA. 106:20069–20074.
Markowitsch HJ, Emmans D, Irle E, Streicher M, Preilowski B. 1985. Cortical and subcortical afferent connections of the primate's temporal pole: a study of rhesus monkeys, squirrel monkeys, and marmosets. J Comp Neurol. 242:425–458.
Marlowe WB, Mancall EL, Thomas JJ. 1975. Complete Kluver-Bucy syndrome in man. Cortex. 11:53–59.

Mathiak KA, Klasen M, Weber R, Ackermann H, Shergill SS, Mathiak K. 2011. Reward system and temporal pole contributions to affective evaluation during a first person shooter video game. BMC Neurosci. 12:66.
Mesulam MM. 2000. Paralimbic (mesocortical) areas. In: Mesulam MM, editor. Principles of behavioral and cognitive neurology. New York: Oxford University Press. p. 49–54.
Mesulam MM, Mufson EJ. 1982. Insula of the old world monkey. III: Efferent cortical output and comments on function. J Comp Neurol. 212:38–52.
Moran MA, Mufson EJ, Mesulam MM. 1987. Neural inputs into the temporopolar cortex of the rhesus monkey. J Comp Neurol. 256:88–103.
Morecraft RJ, Van Hoesen GW. 1998. Convergence of limbic input to the cingulate motor cortex in the rhesus monkey. Brain Res Bull. 45:209–232.
Mufson EJ, Mesulam MM. 1982. Insula of the old world monkey. II: Afferent cortical input and comments on the claustrum. J Comp Neurol. 212:23–37.
Mummery CJ, Patterson K, Price CJ, Ashburner J, Frackowiak RS, Hodges JR. 2000. A voxel-based morphometry study of semantic dementia: relationship between temporal lobe atrophy and semantic memory. Ann Neurol. 47:36–45.
Munoz M, Insausti R. 2005. Cortical efferents of the entorhinal cortex and the adjacent parahippocampal region in the monkey (Macaca fascicularis). Eur J Neurosci. 22:1368–1388.
Murphy K, Bodurka J, Bandettini PA. 2007. How long to scan? The relationship between fMRI temporal signal to noise ratio and necessary scan duration. Neuroimage. 34:565–574.
Murray EA, Bussey TJ, Saksida LM. 2007. Visual perception and memory: a new view of medial temporal lobe function in primates and rodents. Annu Rev Neurosci. 30:99–122.
Murray EA, Richmond BJ. 2001. Role of perirhinal cortex in object perception, memory, and associations. Curr Opin Neurobiol. 11:188–193.
Nakamura K, Kawashima R, Sato N, Nakamura A, Sugiura M, Kato T, Hatano K, Ito K, Fukuda H, Schormann T et al. 2000. Functional delineation of the human occipito-temporal areas related to face and scene processing. A PET study. Brain. 123(Pt 9):1903–1912.
Nakamura K, Kubota K. 1996. The primate temporal pole: its putative role in object recognition and memory. Behav Brain Res. 77:53–77.
Olson IR, Plotzker A, Ezzyat Y. 2007. The enigmatic temporal pole: a review of findings on social and emotional processing. Brain. 130:1718–1731.
Pandya DN, Rosene DL, Doolittle AM. 1994. Corticothalamic connections of auditory-related areas of the temporal lobe in the rhesus monkey. J Comp Neurol. 345:447–471.
Patterson K. 2007. The reign of typicality in semantic memory. Philos Trans R Soc Lond B Biol Sci. 362:813–821.
Patterson K, Nestor PJ, Rogers TT. 2007. Where do you know what you know? The representation of semantic knowledge in the human brain. Nat Rev Neurosci. 8:976–987.
Peelen MV, Caramazza A. 2012. Conceptual object representations in human anterior temporal cortex. J Neurosci. 32:15728–15736.
Petrides M, Pandya DN. 2002. Comparative cytoarchitectonic analysis of the human and the macaque ventrolateral prefrontal cortex and corticocortical connection patterns in the monkey. Eur J Neurosci. 16:291–310.
Petrides M, Pandya DN. 1999. Dorsolateral prefrontal cortex: comparative cytoarchitectonic analysis in the human and the macaque brain and corticocortical connection patterns. Eur J Neurosci. 11:1011–1036.
Petrides M, Pandya DN. 2007. Efferent association pathways from the rostral prefrontal cortex in the macaque monkey. J Neurosci. 27:11573–11586.
Phan TG, Donnan GA, Srikanth V, Chen J, Reutens DC. 2009. Heterogeneity in infarct patterns and clinical outcomes following internal carotid artery occlusion. Arch Neurol. 66:1523–1528.
Pick A. 1905. Zur symptomatologie der linksseitigen Schlafenlappenatrophie. Monatsschr Psychiatr Neurologie. 16:378–388.
Pobric G, Jefferies E, Lambon Ralph MA. 2010. Category-specific versus category-general semantic impairment induced by transcranial magnetic stimulation. Curr Biol. 20:964–968.
Price JL, Drevets WC. 2010. Neurocircuitry of mood disorders. Neuropsychopharmacology. 35:192–216.
Rauschecker JP, Scott SK. 2009. Maps and streams in the auditory cortex: nonhuman primates illuminate human speech processing. Nat Neurosci. 12:718–724.
Regenbogen C, Schneider DA, Gur RE, Schneider F, Habel U, Kellermann T. 2012. Multimodal human communication–targeting facial expressions, speech content and prosody. Neuroimage. 60:2346–2356.
Romanski LM, Bates JF, Goldman-Rakic PS. 1999. Auditory belt and parabelt projections to the prefrontal cortex in the rhesus monkey. J Comp Neurol. 403:141–157.
Royet JP, Zald D, Versace R, Costes N, Lavenne F, Koenig O, Gervais R. 2000. Emotional responses to pleasant and unpleasant olfactory, visual, and auditory stimuli: a positron emission tomography study. J Neurosci. 20:7752–7759.
Saleem KS, Kondo H, Price JL. 2008. Complementary circuits connecting the orbital and medial prefrontal networks with the temporal, insular, and opercular cortex in the macaque monkey. J Comp Neurol. 506:659–693.
Schmahmann JD, Doyon J, McDonald D, Holmes C, Lavoie K, Hurwitz AS, Kabani N, Toga A, Evans A, Petrides M. 1999. Three-dimensional MRI atlas of the human cerebellum in proportional stereotaxic space. Neuroimage. 10:233–260.
Schmahmann JD, Pandya DN. 2006. Fiber pathways of the brain. New York: Oxford University Press.
Schmahmann JD, Pandya DN. 1991. Projections to the basis pontis from the superior temporal sulcus and superior temporal region in the rhesus monkey. J Comp Neurol. 308:224–248.
Schwartz MF, Kimberg DY, Walker GM, Brecher A, Faseyitan OK, Dell GS, Mirman D, Coslett HB. 2011. Neuroanatomical dissociation for taxonomic and thematic knowledge in the human brain. Proc Natl Acad Sci USA. 108:8520–8524.
Schwartz MF, Kimberg DY, Walker GM, Faseyitan O, Brecher A, Dell GS, Coslett HB. 2009. Anterior temporal involvement in semantic word retrieval: voxel-based lesion-symptom mapping evidence from aphasia. Brain. 132:3411–3427.
Seltzer B, Pandya DN. 1989. Intrinsic connections and architectonics of the superior temporal sulcus in the rhesus monkey. J Comp Neurol. 290:451–471.
Seltzer B, Pandya DN. 1994. Parietal, temporal, and occipital projections to cortex of the superior temporal sulcus in the rhesus monkey: a retrograde tracer study. J Comp Neurol. 343:445–463.
Sharp DJ, Scott SK, Wise RJ. 2004. Retrieving meaning after temporal lobe infarction: the role of the basal language area. Ann Neurol. 56:836–846.
Shin LM, Dougherty DD, Orr SP, Pitman RK, Lasko M, Macklin ML, Alpert NM, Fischman AJ, Rauch SL. 2000. Activation of anterior paralimbic structures during guilt-related script-driven imagery. Biol Psychiatry. 48:43–50.
Simmons WK, Reddish M, Bellgowan PS, Martin A. 2010. The selectivity and functional connectivity of the anterior temporal lobes. Cereb Cortex. 20:813–825.
Skipper LM, Ross LA, Olson IR. 2011. Sensory and semantic category subdivisions within the anterior temporal lobes. Neuropsychologia. 49:3419–3429.
Smith GE. 1907. A new topographical survey of the human cerebral cortex, being an account of the distribution of the anatomically distinct cortical areas and their relationship to the cerebral sulci. J Anat Physiol. 41:237–254.
Stefanacci L, Suzuki WA, Amaral DG. 1996. Organization of connections between the amygdaloid complex and the perirhinal and parahippocampal cortices in macaque monkeys. J Comp Neurol. 375:552–582.
Stoodley CJ, Schmahmann JD. 2010. Evidence for topographic organization in the cerebellum of motor control versus cognitive and affective processing. Cortex. 46:831–844.

Stoodley CJ, Valera EM, Schmahmann JD. 2010. An fMRI study of intra-individual functional topography in the human cerebellum. Behav Neurol. 23:65–79.
Tada M, Kakita A, Toyoshima Y, Onodera O, Ozawa T, Morita T, Nishizawa M, Takahashi H. 2009. Depletion of medullary serotonergic neurons in patients with multiple system atrophy who succumbed to sudden death. Brain. 132:1810–1819.
Teki S, Chait M, Kumar S, von Kriegstein K, Griffiths TD. 2011. Brain bases for auditory stimulus-driven figure-ground segregation. J Neurosci. 31:164–171.
Thesen T, McDonald CR, Carlson C, Doyle W, Cash S, Sherfey J, Felsovalyi O, Girard H, Barr W, Devinsky O et al. 2012. Sequential then interactive processing of letters and words in the left fusiform gyrus. Nat Commun. 3:1284.
Thompson PM, Hayashi KM, de Zubicaray G, Janke AL, Rose SE, Semple J, Herman D, Hong MS, Dittmer SS, Doddrell DM et al. 2003. Dynamics of gray matter loss in Alzheimer's disease. J Neurosci. 23:994–1005.
Tillfors M, Furmark T, Marteinsdottir I, Fischer H, Pissiota A, Langstrom B, Fredrikson M. 2001. Cerebral blood flow in subjects with social phobia during stressful speaking tasks: a PET study. Am J Psychiatry. 158:1220–1226.
Tsapkini K, Frangakis CE, Hillis AE. 2011. The function of the left anterior temporal pole: evidence from acute stroke and infarct volume. Brain. 134:3094–3105.
Tsukiura T, Mochizuki-Kawai H, Fujii T. 2006. Dissociable roles of the bilateral anterior temporal lobe in face-name associations: an event-related fMRI study. Neuroimage. 30:617–626.
Van Dijk KR, Hedden T, Venkataraman A, Evans KC, Lazar SW, Buckner RL. 2010. Intrinsic functional connectivity as a tool for human connectomics: theory, properties, and optimization. J Neurophysiol. 103:297–321.
Van Hoesen GW, Yeterian EH, Lavizzo-Mourey R. 1981. Widespread corticostriate projections from temporal cortex of the rhesus monkey. J Comp Neurol. 199:205–219.
Vincent JL, Snyder AZ, Fox MD, Shannon BJ, Andrews JR, Raichle ME, Buckner RL. 2006. Coherent spontaneous activity identifies a hippocampal-parietal memory network. J Neurophysiol. 96:3517–3531.
Visser M, Jefferies E, Embleton KV, Lambon Ralph MA. 2012. Both the middle temporal gyrus and the ventral anterior temporal area are crucial for multimodal semantic processing: distortion-corrected fMRI evidence for a double gradient of information convergence in the temporal lobes. J Cogn Neurosci. 24:1766–1778.
Visser M, Lambon Ralph MA. 2011. Differential contributions of bilateral ventral anterior temporal lobe and left anterior superior temporal gyrus to semantic processes. J Cogn Neurosci. 23:3121–3131.
Von Bonin G, Bailey P. 1947. The neocortex of Macaca mulatta. Urbana: University of Illinois Press.
Von Economo C. 1929. The cytoarchitectonics of the human cerebral cortex. London: Oxford University Press.
Von Economo C, Koskinas GN. 1925. Die Cytoarchitecktonik der Grosshirnrinde des erwachsenen Menschen. Berlin: Springer.
Webster MJ, Ungerleider LG, Bachevalier J. 1991. Connections of inferior temporal areas TE and TEO with medial temporal-lobe structures in infant and adult monkeys. J Neurosci. 11:1095–1116.
Wilson SM, Henry ML, Besbris M, Ogar JM, Dronkers NF, Jarrold W, Miller BL, Gorno-Tempini ML. 2010. Connected speech production in three variants of primary progressive aphasia. Brain. 133:2069–2088.
Yeo BT, Krienen FM, Sepulcre J, Sabuncu MR, Lashkari D, Hollinshead M, Roffman JL, Smoller JW, Zollei L, Polimeni JR et al. 2011. The organization of the human cerebral cortex estimated by intrinsic functional connectivity. J Neurophysiol. 106:1125–1165.
Yeterian EH, Pandya DN. 1998. Corticostriatal connections of the superior temporal region in rhesus monkeys. J Comp Neurol. 399:384–402.
Yeterian EH, Pandya DN. 1991. Corticothalamic connections of the superior temporal sulcus in rhesus monkeys. Exp Brain Res. 83:268–284.
Yeterian EH, Pandya DN. 1989. Thalamic connections of the cortex of the superior temporal sulcus in the rhesus monkey. J Comp Neurol. 282:80–97.
Zahn R, Moll J, Krueger F, Huey ED, Garrido G, Grafman J. 2007. Social concepts are represented in the superior anterior temporal cortex. Proc Natl Acad Sci USA. 104:6430–6435.
Zec N, Filiano JJ, Kinney HC. 1997. Anatomic relationships of the human arcuate nucleus of the medulla: a DiI-labeling study. J Neuropathol Exp Neurol. 56:509–522.